

# Marine Ecosystems

SOUTH  
AUSTRALIAN  
RESEARCH &  
DEVELOPMENT  
INSTITUTE  
**PIRSA**

## Analysis of the sea-state in Sleaford Bay, South Australia



**Charles James and Mark Doubell**

**SARDI Publication No. F2020/000517-1  
SARDI Research Report Series No. 1083**

**SARDI Aquatics Sciences  
PO Box 120 Henley Beach SA 5022**

**February 2021**

**Report to SA Water**



# **Analysis of the sea-state in Sleaford Bay, South Australia**

**Report to SA Water**

**Charles James and Mark Doubell**

**SARDI Publication No. F2020/000517-1  
SARDI Research Report Series No. 1083**

**February 2021**

This publication may be cited as:

James, C. and Doubell, M. (2021). Analysis of the sea-state in Sleaford Bay, South Australia. Report to SA Water. South Australian Research and Development Institute (Aquatic Sciences), Adelaide. SARDI Publication No. F2020/000517-1. SARDI Research Report Series No. 1083. 42pp.

**South Australian Research and Development Institute**

SARDI Aquatic Sciences

2 Hamra Avenue

West Beach SA 5024

Telephone: (08) 8207 5400

Facsimile: (08) 8207 5415

<http://www.pir.sa.gov.au/research>

**DISCLAIMER**

The authors warrant that they have taken all reasonable care in producing this report. The report has been through the SARDI internal review process, and has been formally approved for release by the Research Director, Aquatic Sciences. Although all reasonable efforts have been made to ensure quality, SARDI does not warrant that the information in this report is free from errors or omissions. SARDI and its employees do not warrant or make any representation regarding the use, or results of the use, of the information contained herein as regards to its correctness, accuracy, reliability and currency or otherwise. SARDI and its employees expressly disclaim all liability or responsibility to any person using the information or advice. Use of the information and data contained in this report is at the user's sole risk. If users rely on the information they are responsible for ensuring by independent verification its accuracy, currency or completeness. The SARDI Report Series is an Administrative Report Series which has not been reviewed outside the department and is not considered peer-reviewed literature. Material presented in these Administrative Reports may later be published in formal peer-reviewed scientific literature.

**© 2021 SARDI**

This work is copyright. Apart from any use as permitted under the *Copyright Act 1968 (Cth)*, no part may be reproduced by any process, electronic or otherwise, without the specific written permission of the copyright owner. Neither may information be stored electronically in any form whatsoever without such permission.

SARDI Publication No. F2020/000517-1  
SARDI Research Report Series No. 1083

Author(s): Charles James and Mark Doubell

Reviewer(s): Roger Kirkwood and Jason Tanner

Approved by: A/Prof Tim Ward

Signed: 

Date: 8 February 2021

Distribution: SA Water, SARDI Aquatic Sciences, Parliamentary Library, State Library and National Library

Circulation: Public Domain

## TABLE OF CONTENTS

ACKNOWLEDGEMENTS .....	VIII
EXECUTIVE SUMMARY .....	1
1 INTRODUCTION .....	2
1.1 Background.....	2
1.2 Objectives.....	2
2 METHODS.....	3
2.1 Study Location.....	3
2.2 Ocean model time-series analysis .....	4
2.3 <i>In situ</i> wave and current observations.....	5
3 RESULTS & DISCUSSION.....	7
3.1 Time-series analysis .....	7
3.1.1 Waves: Cape du Couedic observations vs CAWCR model.....	7
3.1.2 Waves: Annual analysis.....	8
3.1.3 Waves: Seasonal analysis .....	12
3.1.4 Wind: Annual analysis.....	18
3.1.5 Wind: Seasonal analysis.....	22
3.1.6 Wave height (Hs) versus wave period (Tp) .....	29
3.1.7 Current Analysis .....	30
3.2 <i>In situ</i> mooring observations .....	33
3.2.1 Waves.....	33
3.2.2 Currents.....	35
4 CONCLUSIONS.....	38
5 REFERENCES .....	40
6 APPENDIX.....	41

## LIST OF FIGURES

<b>Figure 1:</b> Regional map showing the locations of the proposed desalination plant (blue marker) in Sleaford Bay and modelled oceanographic data collection grid-points (Centre for Australian Weather and Climate Research, CAWCR). CAWCR model grid points used in the analyses were Sleaford Bay (green triangle) and Cape du Couedic (green circle).....	3
<b>Figure 2:</b> Image from cruise plan showing close-up of the mooring location (red circle) in relation to the proposed desalination plant site, including the region for the outfall region (green circle). Grey lines indicate bathymetric contours at 5 m intervals starting at 10 m. The oceanographic mooring is located in approximately 20 m of water.....	4
<b>Figure 3:</b> The oceanographic mooring being readied for deployment. An Acoustic Doppler Current Profiler (ADCP) is on the right, a Conductivity, Temperature, Depth sensor (CTD) is on the left and the (yellow) acoustic release float pack is in the front and centre. ....	6
<b>Figure 4:</b> Comparison between model output and observations at the site of the Bureau of Meteorology’s Cape du Couedic WaveRider mooring for the period June 2012 to June 2013....	7
<b>Figure 5:</b> Return periods (years) for extreme significant wave heights at Sleaford Bay (top) and Cape du Couedic (bottom). ....	8
<b>Figure 6:</b> Significant wave height ( $H_s$ ) histogram as a function of mean wave direction at Sleaford Bay (left) and Cape du Couedic (right). ....	9
<b>Figure 7:</b> Significant wave height ( $H_s$ ) below threshold values at Sleaford Bay (top) and Cape du Couedic (bottom). ....	10
<b>Figure 8:</b> Number of days per year with significant wave heights ( $H_s$ ) less than threshold values at Sleaford Bay (top) and Cape du Couedic (bottom). ....	11
<b>Figure 9:</b> Return periods (years) for peak wave period ( $T_p$ ) at Sleaford Bay (top) and Cape du Couedic (bottom). ....	12
<b>Figure 10:</b> Return period (yrs) of extreme significant wave height ( $H_s$ ) events by season at Sleaford Bay. ....	13
<b>Figure 11:</b> Return period (yrs) of extreme significant wave height ( $H_s$ ) events by season at Cape du Couedic.....	14
<b>Figure 12:</b> Sleaford Bay: seasonal significant wave height ( $H_s$ ) as a function of wave direction. ....	15
<b>Figure 13:</b> Cape du Couedic: seasonal significant wave height ( $H_s$ ) as a function of wave direction. ....	16
<b>Figure 14:</b> Seasonal threshold analysis of significant wave height ( $H_s$ ) at Sleaford Bay.....	17

<b>Figure 15:</b> Numbers of days with significant wave heights ( $H_s$ ) below threshold values, by season at Sleaford Bay. ....	18
<b>Figure 16:</b> Return periods for extreme wind speeds ( $W$ ) at analysis sites.....	19
<b>Figure 17:</b> Wind speed ( $W$ ) histograms as a function of direction for Sleaford Bay (left) and Cape du Couedic.....	20
<b>Figure 18:</b> Frequency of wind speeds ( $W$ ) below thresholds of 30, 20, 15 and 10 knots (55.6, 37.0, 27.8, and 18.5 km/h) for Sleaford Bay (top) and Cape du Couedic (bottom).....	21
<b>Figure 19:</b> Number of days per year with wind speeds ( $W$ ) less than thresholds of 30, 20, 15 and 10 knots (55.6, 37.0, 27.8, and 18.5 km/h) for Sleaford Bay (top) and Cape du Couedic (bottom). ....	22
<b>Figure 20:</b> Return periods for extreme wind speeds ( $W$ ) by season at Sleaford Bay.....	23
<b>Figure 21:</b> Return periods for extreme wind speeds ( $W$ ) by season at Cape du Couedic. ....	24
<b>Figure 22:</b> Wind speed ( $W$ ) as a function of wind direction at Sleaford Bay. ....	25
<b>Figure 23:</b> Wind speed ( $W$ ) as a function of wind direction at Cape du Couedic. ....	26
<b>Figure 24:</b> Seasonal Threshold analysis of wind speed ( $W$ ) at Sleaford Bay. ....	27
<b>Figure 25:</b> Number of days with winds below threshold values, by season at Sleaford Bay (total days for summer=90, autumn=92, winter=92, and spring=91).....	28
<b>Figure 26:</b> Scatter plot of modelled significant wave height ( $H_s$ ) against peak wave period ( $T_p$ ) at Sleaford Bay. ....	30
<b>Figure 27:</b> Location, speed and direction of modelled ocean currents at Sleaford Bay. The map indicates the location of the mooring site relative to the CAWCR and TGM modelled grid-points. ....	31
<b>Figure 28:</b> Location, speed and direction of modelled tidal currents at Sleaford Bay. The map indicates the location of the mooring site relative to the CAWCR and TGM modelled grid-points. ....	32
<b>Figure 29:</b> Seasonal current patterns within Sleaford Bay based on averages for 2016-2018. .	33
<b>Figure 30:</b> Observations of significant wave height ( $H_s$ ) and peak period ( $T_p$ ) measured by the moored ADCP.....	34
<b>Figure 31:</b> Average directional wave spectrum measured by the Acoustic Doppler Current Profiler (ADCP) in Sleaford Bay. ....	35
<b>Figure 32:</b> Depth-averaged current speeds and directions measured by the Acoustic Doppler Current Profiler (ADCP) in Sleaford Bay. The map indicates the location of the mooring site relative to the CAWCR and TGM modelled grid-points.....	36

<b>Figure 33:</b> Tide filtered depth-averaged current speeds and directions measured by the Acoustic Doppler Current Profiler (ADCP) in Sleaford Bay. The map indicates the location of the mooring site relative to the CAWCR and TGM modelled grid-points .....	37
<b>Figure 34:</b> Correlation and linear regression through the origin of maximum wave height ( $H_{max}$ ) as a function of significant wave height ( $H_s$ ) at a site in the Great Australian Bight (GAB) (left) and the Cape du Couedic WaveRider mooring. ....	41
<b>Figure 35:</b> Top row: histograms of ratio of maximum wave height ( $H_{max}$ ) to significant wave height ( $H_s$ ) ( $R = H_{max}/H_s$ ) for model (Great Australian Bight, GAB) and observation (Cape du Couedic) sites. Bottom row: averaged $R$ plotted as a function of $H_s$ in 0.5 m bins, error bars indicate +/- one standard deviation ( $\sigma$ ). ....	42

## LIST OF TABLES

<b>Table 1:</b> Summary of return-period heights for significant wave heights ( $H_s$ , in m) at Sleaford Bay and Cape du Couedic. ....	13
<b>Table 2:</b> Summary of return-period wind speeds ( $W$ ) for maximum winds (km/h) at Sleaford Bay and Cape du Couedic. ....	22
<b>Table 3:</b> Distribution of significant wave height ( $H_s$ ) versus peak wave period ( $T_p$ ) at Sleaford Bay: indicated are the percentage of waves with characteristics lying within 0.5 m x 2 s bins. ...	29

## **ACKNOWLEDGEMENTS**

Thank you to the SARDI staff Paul Malthouse, David Delaine, Ben Stobart and Katherine Heldt for their professionalism and efforts in the preparation, deployment and recovery of the oceanographic mooring.



## EXECUTIVE SUMMARY

To secure future regional water supplies on Eyre Peninsula, SA Water proposes to build a desalination plant at Sleaford Bay located approximately 20 km south-west of Port Lincoln. The proposed location is exposed to energetic oceanic conditions that are expected to rapidly disperse the saline outflow from the desalination plant. Prior to development, an understanding of the sea conditions in Sleaford Bay is needed to assess potential impacts on engineered structures associated with the desalination plant.

Currently, there are no long-term observations of winds, waves or currents in Sleaford Bay to characterise the local environment and estimate 100-year return values for extreme wind and wave events. To fill this observational gap, data from wave and hydrodynamic computer models are analysed. Results indicate waves entering Sleaford Bay are predominately from the south-west year-round, with significant wave heights below 3.5 m occurring 99.2% of the time with a 100-year return height of 6.7 m. Peak wave periods have a 100-year return period of 28.9 s. Winds varied seasonally, with summer south-easterlies and winter south-westerlies, and a 100-year return speed of 83.8 km/h (45.2 knots). Maximum depth-averaged current speeds were approximately 20 cm/s and were orientated along a north-east/south-west axis. Model circulation indicates the presence of a counter-clockwise eddy within Sleaford Bay. Model results were /supplemented by 46 days of direct measurements of waves and currents in spring 2020. Recorded significant wave heights remained below 2.5 m with a maximum peak-period of 17 s. Wave directions were predominantly from the south-east as a result of refraction due to interactions with local bathymetry. Observed depth-averaged current speeds remained below 20 cm/s and were orientated along isobaths with a north–south axis. These findings provide a clearer understanding of the ocean conditions likely to be encountered in Sleaford Bay.

**Keywords:** Sleaford Bay, sea-state, oceanography, wind, waves, currents, return periods, extreme events, ocean model.

# 1 INTRODUCTION

## 1.1 Background

Security of regional water supplies is a key priority for SA Water. Existing water supplies for regional communities on Eyre Peninsula need to be supplemented to ensure future proofing. To achieve this, SA Water proposes to build a desalination plant at Sleaford Bay, approximately 20 km south-west of Port Lincoln. The proposed location of the desalination plant's outfall and intake structures is at the western end of Sleaford Bay. Whilst the energetic oceanic conditions at the proposed site are expected to rapidly disperse the saline waste stream, they also have potential to impact on any engineered structures associated with the plant.

To support the development of the desalination plant, an understanding of the sea-state conditions in Sleaford Bay is required. Due to an absence of long time-series of oceanographic and meteorological observations in Sleaford Bay, this study presents results from a statistical analysis of time-series generated by global and regional models for wind, waves and currents. Model results are used to characterise the sea-state in Sleaford Bay and estimate 100-year return values for extreme events. In addition, *in situ* observations of waves and currents from a short-term mooring deployment at the proposed site in Sleaford Bay are summarised. The direct observations allow for validation of the model results and an improved understanding of how local processes, not captured by the models, influence the wave and current climate experienced at the site.

## 1.2 Objectives

1. Provide a quantitative summary of the sea-state in Sleaford Bay and determine the probability of extreme events for wind and waves based on using long-term time-series of wind, wave and ocean currents from regional and global ocean models.
2. Deploy and recover an ocean mooring in Sleaford Bay and summarise the *in situ* current and wave observations.

## 2 /METHODS

### 2.1 Study Location

The location of proposed Sleaford desalination site (blue diamond,  $135^{\circ} 42.4225$  East,  $34^{\circ} 53.0074'$  South), the mooring (red star,  $135^{\circ} 42.7460'$  East,  $34^{\circ} 53.2333'$  South) and modelled oceanographic data-collection grid-points are shown in Figure 1 and Figure 2.

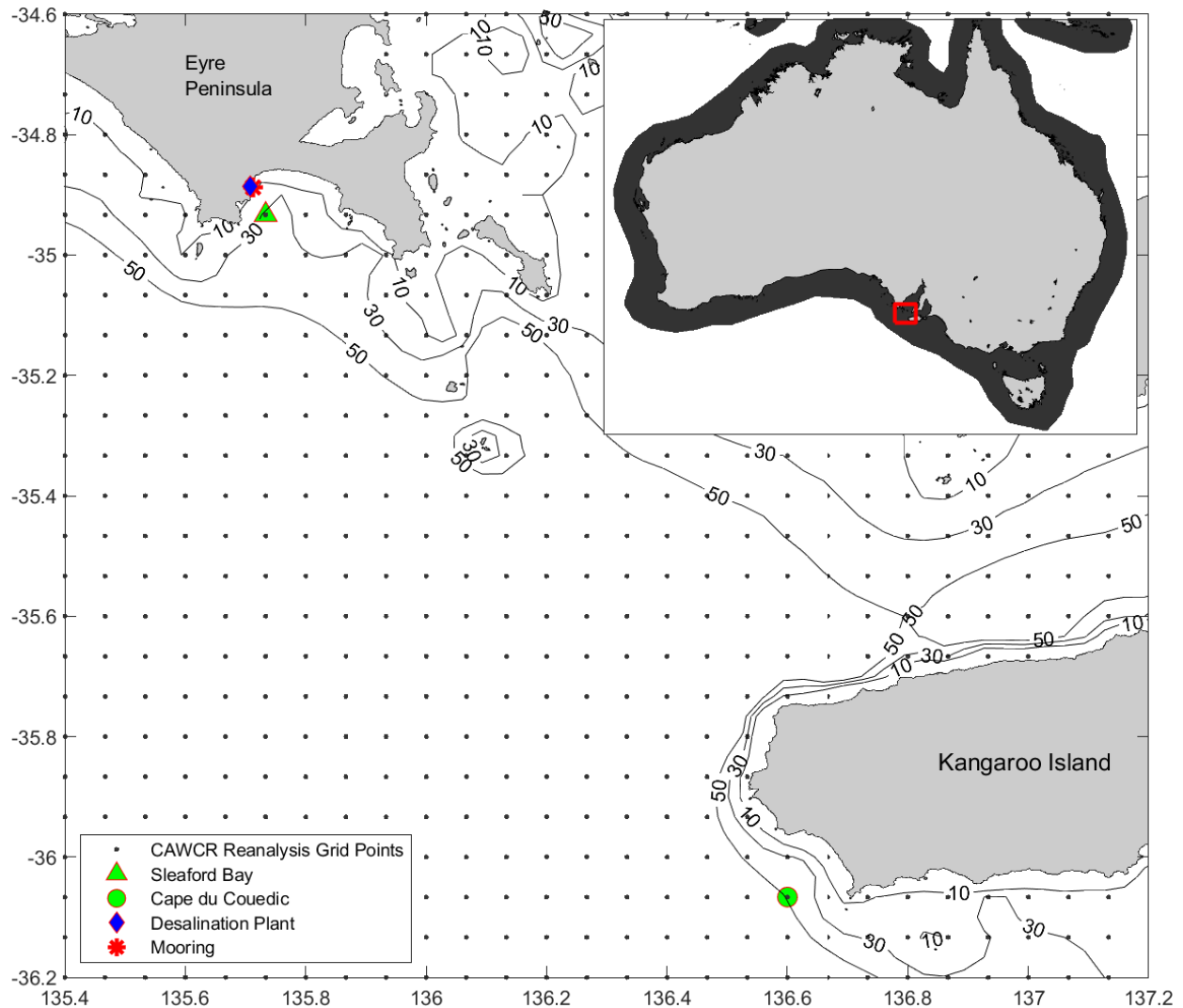


**Figure 1:** Regional map showing the locations of the proposed desalination plant (blue marker) in Sleaford Bay and modelled oceanographic data collection grid-points (Centre for Australian Weather and Climate Research, CAWCR). CAWCR model grid points used in the analyses were Sleaford Bay (green triangle) and Cape du Couedic (green circle).



**Figure 2:** Image from cruise plan showing close-up of the mooring location (red circle) in relation to the proposed desalination plant site, including the region for the outfall region (green circle). Grey lines indicate bathymetric contours at 5 m intervals starting at 10 m. The oceanographic mooring is located in approximately 20 m of water.

## 2.2 Ocean model time-series analysis

For analysis and characterization of wave and wind properties and the determination of the 100-year return values, the Centre for Australian Weather and Climate Research (CAWCR) Wave hindcasts and extensions (Durrant et al. 2014) were used to provide hourly averaged output covering the period from January 1979 to January 2014. For the ocean currents, vertically averaged output from a tide-resolving 1.5 km resolution version of the eSA-Marine 2-Gulf model (Rogers et al., 2020, [https://www.pir.sa.gov.au/research/esa\\_marine](https://www.pir.sa.gov.au/research/esa_marine)) run for a period of 3 years (2016-2018) was used, hereafter referred to as the TGM.

In Sleaford Bay, the model cell nearest the desalination site was selected (Figure 1, green triangle). Wave model results were compared with existing Bureau of Meteorology WaveRider Buoy data collected off Cape du Couedic on the south west coast of Kangaroo Island (Figure 1, green circle). The hydrodynamic model cell was chosen as the closest cell to the wave analysis cell within Sleaford Bay. The high resolution of the TGM model meant the hydrodynamic model

cell was essentially indistinguishable from the CAWCR wave cell (see Figure 27 for example) and both sites are referred to as Sleaford Bay hereafter.

The wave, wind and ocean current parameters investigated were:

- $H_s$  – significant wave height – the average of the highest one-third of waves in the wave spectrum, considered to be the best estimate of the wave field (Sverdrup and Munk 1947).
- $H_{max}$  – maximum wave height.
- $T_p$  – peak wave period – is the wave period of the most energetic waves within the dominant swell waves.
- $D_m$  – mean wave direction – estimates are based on the direction of the waves averaged over the entire spectrum.
- $W$  – magnitude of wind vector at 10 m –used to perform the return-period analysis for wind speeds.
- $\bar{V}$  – vertically averaged components of the current.

Return values for  $H_s$ ,  $T_p$ , and  $W$  were calculated using the Gringorten method (Gringorten 1963) and based on modelling the tail of a Gumbel distribution applied to the probability distribution of yearly maximum values. Return values were calculated for 10, 25 and 100-year periods. Seasonal return values were estimated by forming the probability distribution from the maximum parameter value for each season over the model duration. Since the maximum value may occur in different seasons in different years the seasonal return values will not be greater than, and are usually less than, the annual return values which are always estimated using the maximum value for each year. A directional return-period analysis was applied to  $H_s$  as a function of  $D_m$ .

The frequency of occurrence of days when  $H_s$  and  $W$  were below certain thresholds were assessed. Threshold  $H_s$  levels were, 4.5, 3.5, 2.5 and 1.5 m, while threshold  $W$  levels were, 30, 20, 15, and 10 knots (i.e. 55.6, 37.0, 27.8, and 18.5 km/h). Estimates of the number of days each year when the wave sea-state and wind speeds remained below each of the thresholds were calculated from model time series.

### **2.3 *In situ* wave and current observations**

An oceanographic mooring was installed in Sleaford Bay adjacent to the proposed desalination plant (Figure 1). The oceanographic mooring consisted of a Nortek Signature 1000 Acoustic

Doppler Current Profiler (ADCP) and a Conductivity Temperature Depth sensor (CTD) mounted on a triangular frame (Figure 3). The ADCP and CTD sensors were located approximately 50 cm and 120 cm above the seafloor. The mooring was deployed on the bottom at approximately 20 m on 11-September 2020 and recovered 47 days later on 28-October. The CTD was supplied by SA Water and the data it collected are not included in this report.

Data collected by the ADCP included 20-minute average measures of the horizontal current speed (U and V – components) throughout the water column in 1 m bins. Horizontal components were vector-averaged and depth-averaged to derive corresponding estimates of current speed and direction. Hourly wave measurements were determined from 17-min. sampling bursts. Custom software (Nortek ‘Ocean Contour’) was used to process the ADCP data and generate the wave parameters ( $H_s$ ,  $H_{max}$ ,  $T_p$ ) and the 2-dimensional wave spectrum.



**Figure 3:** The oceanographic mooring being readied for deployment. An Acoustic Doppler Current Profiler (ADCP) is on the right, a Conductivity, Temperature, Depth sensor (CTD) is on the left and the (yellow) acoustic release float pack is in the front and centre.

### 3 RESULTS & DISCUSSION

#### 3.1 Time-series analysis

##### 3.1.1 Waves: Cape du Couedic observations vs CAWCR model

The Bureau of Meteorology WaveRider Buoy at Cape du Couedic has been operating since November 2000. The observational time-series has several significant breaks in measurement (due to maintenance issues) and the time-series is too short for an accurate 100-year return-period analysis. The CAWCR model is a reanalysis and assimilates wave observations from Cape du Couedic, where available, into the model run. Comparison of a year-long uninterrupted sequence of buoy observations with the CAWCR output showed a reasonably strong correlation ( $r = 0.72$ ; Figure 4). It should be noted that the model produced slightly larger significant wave heights, with an overall bias of 30-40 cm, so extreme values based on model runs tend to be slightly overestimated.

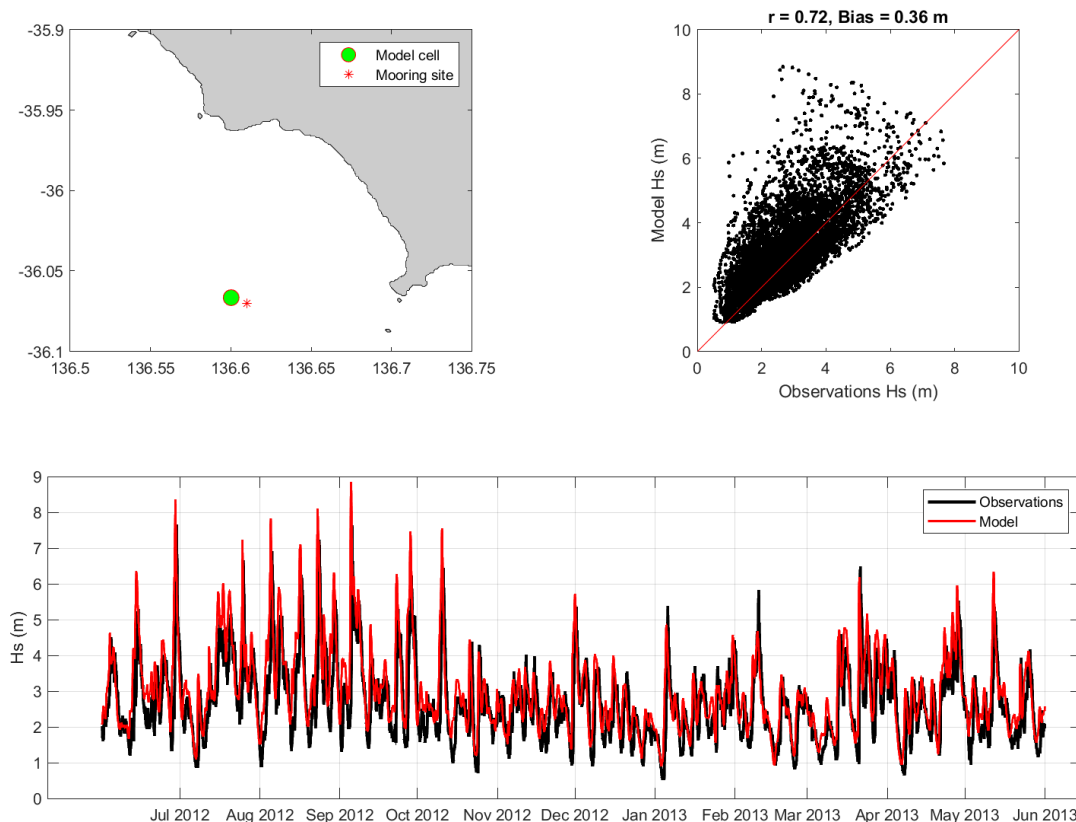


**Figure 4:** Comparison between model output and observations at the site of the Bureau of Meteorology's Cape du Couedic WaveRider mooring for the period June 2012 to June 2013.

### 3.1.2 Waves: Annual analysis

The CAWCR wave model does not provide a maximum wave height value ( $H_{max}$ ) so the following analysis was based on  $H_s$ . For this region, an estimate of  $H_{max}$  can be obtained by multiplying  $H_s$  by a scaling factor of 1.6 (see Appendix for analysis and discussion of this estimate).

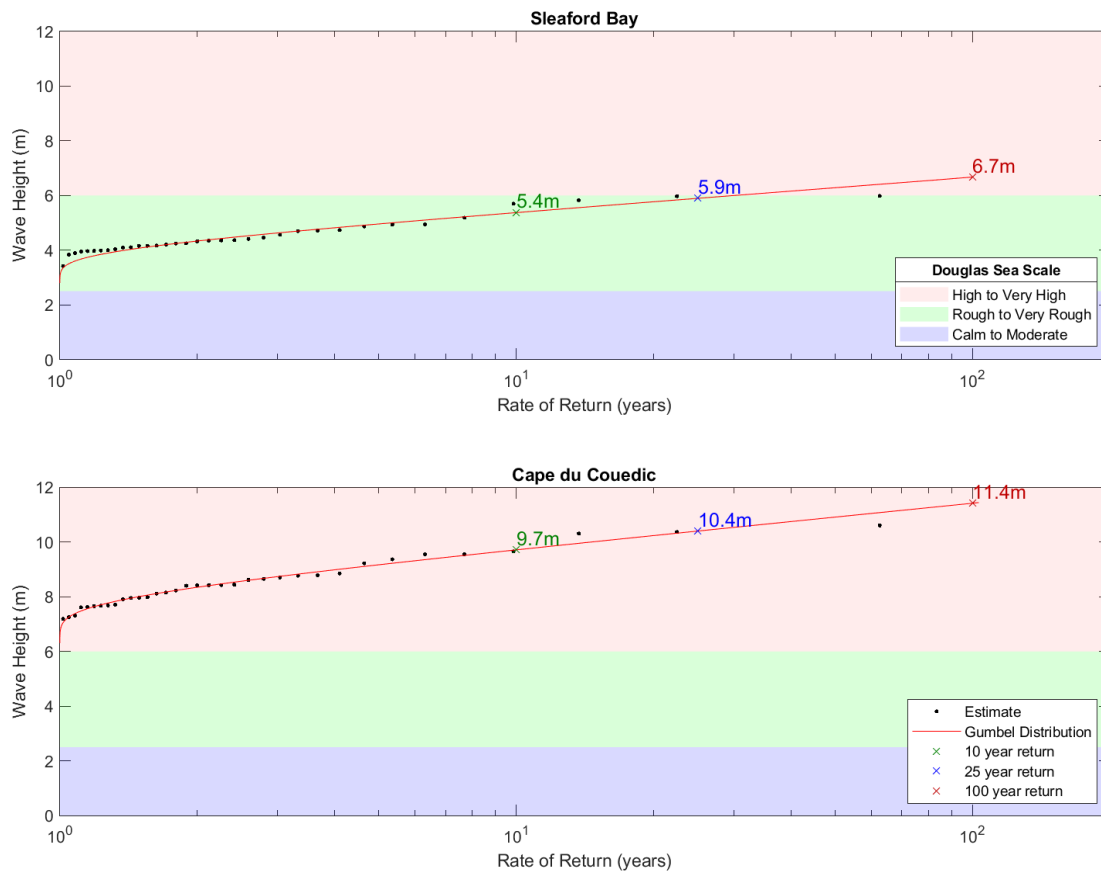


**Figure 5:** Return periods (years) for extreme significant wave heights at Sleaford Bay (top) and Cape du Couedic (bottom).

The 100-year return heights for  $H_s$  at Sleaford Bay and Cape du Couedic were 6.7 m and 11.4 m, respectively (Figure 5). The Sleaford Bay site is significantly more sheltered than the Cape du Couedic site so lower extreme values for  $H_s$  are to be expected. Broken down by direction, the dominant nature of the swell is apparent, originating in the Southern Ocean and arriving from the south-west (Figure 6).



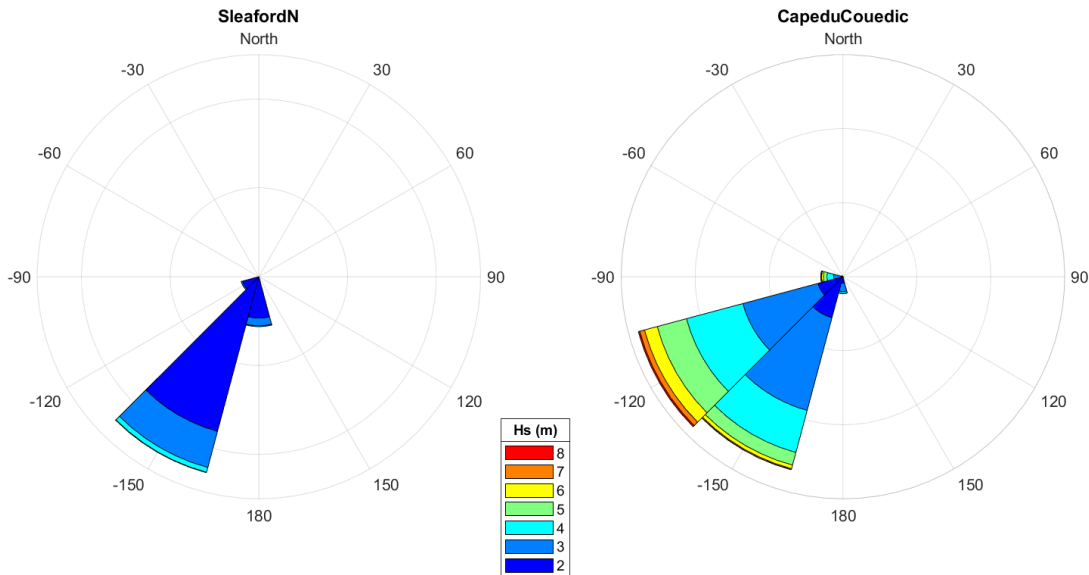


**Figure 6:** Significant wave height ( $H_s$ ) histogram as a function of mean wave direction at Sleaford Bay (left) and Cape du Couedic (right).

It is also of interest to estimate the inter-annual frequency with which particular sea-states occur. The wave model output over a 30+ year period highlights four arbitrary levels of  $H_s$  (1.5, 2.5, 3.5, and 4.5 m) that delineate a decreasing ability of vessels to perform operations safely (Figure 6). The percentage of modelled wave data points that fall below these thresholds is indicated next to the plot. Another way to look at this data is to show, on average, how many days out of each year the sea-state will be below these levels (Figure 7). Because of the exposed nature of Cape du Couedic there are far fewer days on average each year where  $H_s$  is below 1.5m than in Sleaford Bay (11 days vs. 191 days). The 100-year return period of  $T_p$  are 28.9 s and 29.1 s for Sleaford Bay and Cape du Couedic respectively (Figure 9). The values are relatively consistent between sites and return periods, reflecting the dominant swell characteristics of waves entering the region.

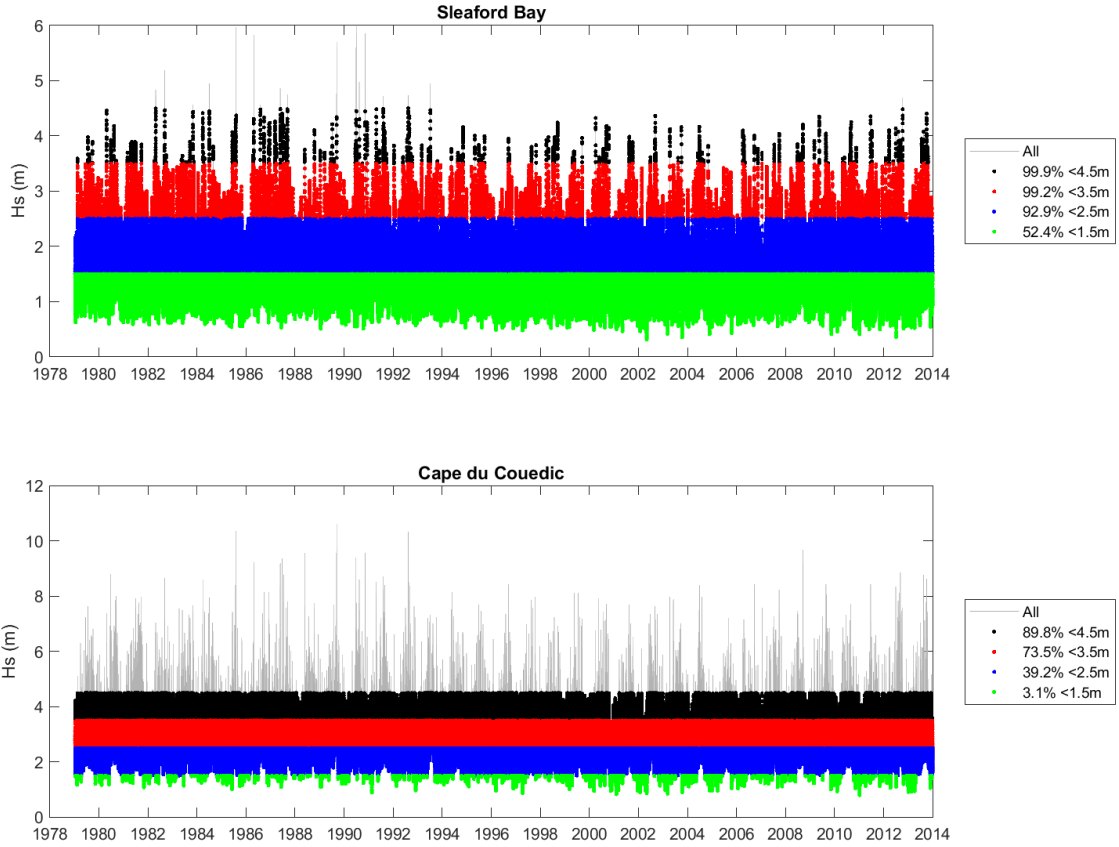


**Figure 7:** Significant wave height (Hs) below threshold values at Sleaford Bay (top) and Cape du Couedic (bottom).

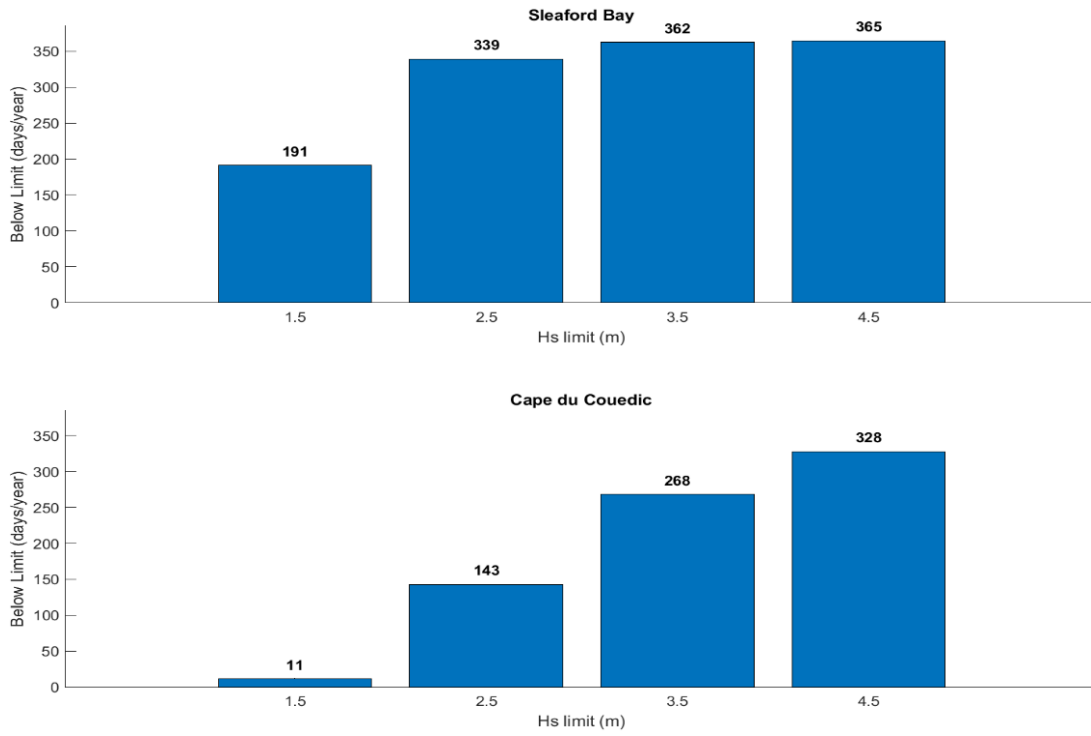


**Figure 8:** Number of days per year with significant wave heights (Hs) less than threshold values at Sleaford Bay (top) and Cape du Couedic (bottom).

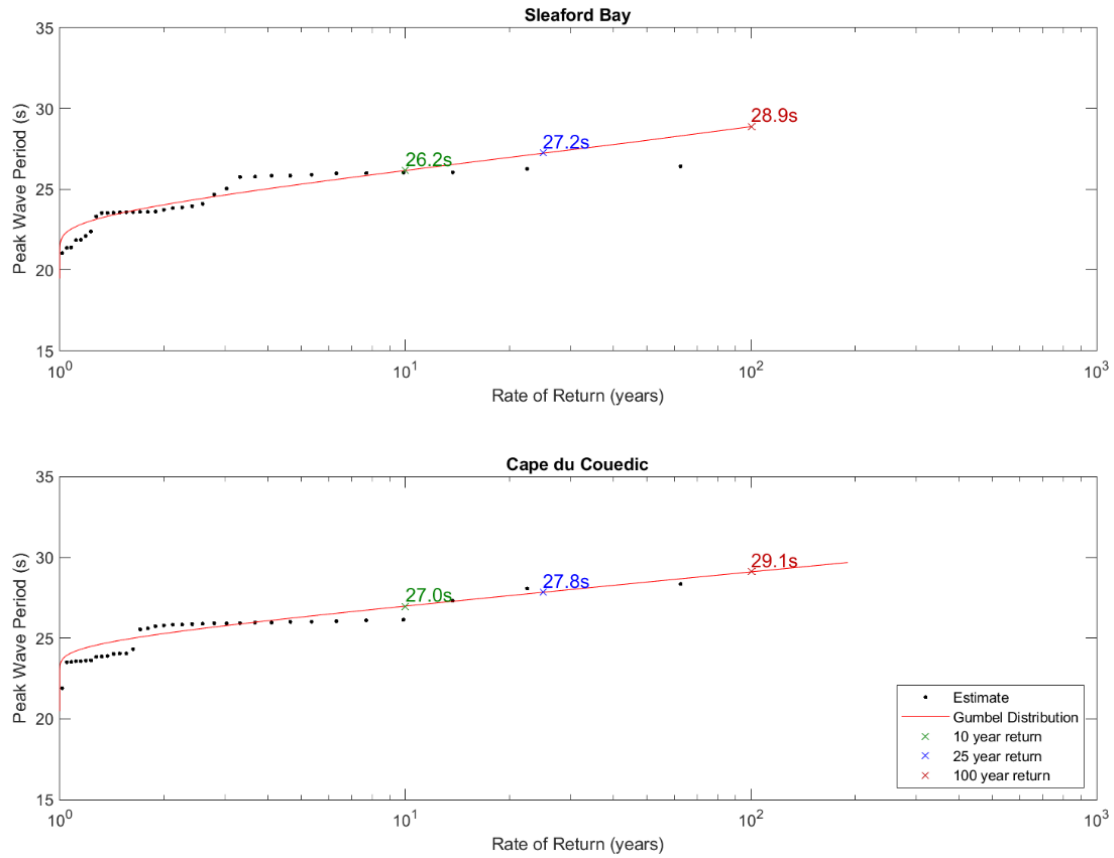


**Figure 9:** Return periods (years) for peak wave period ( $T_p$ ) at Sleaford Bay (top) and Cape du Couedic (bottom).

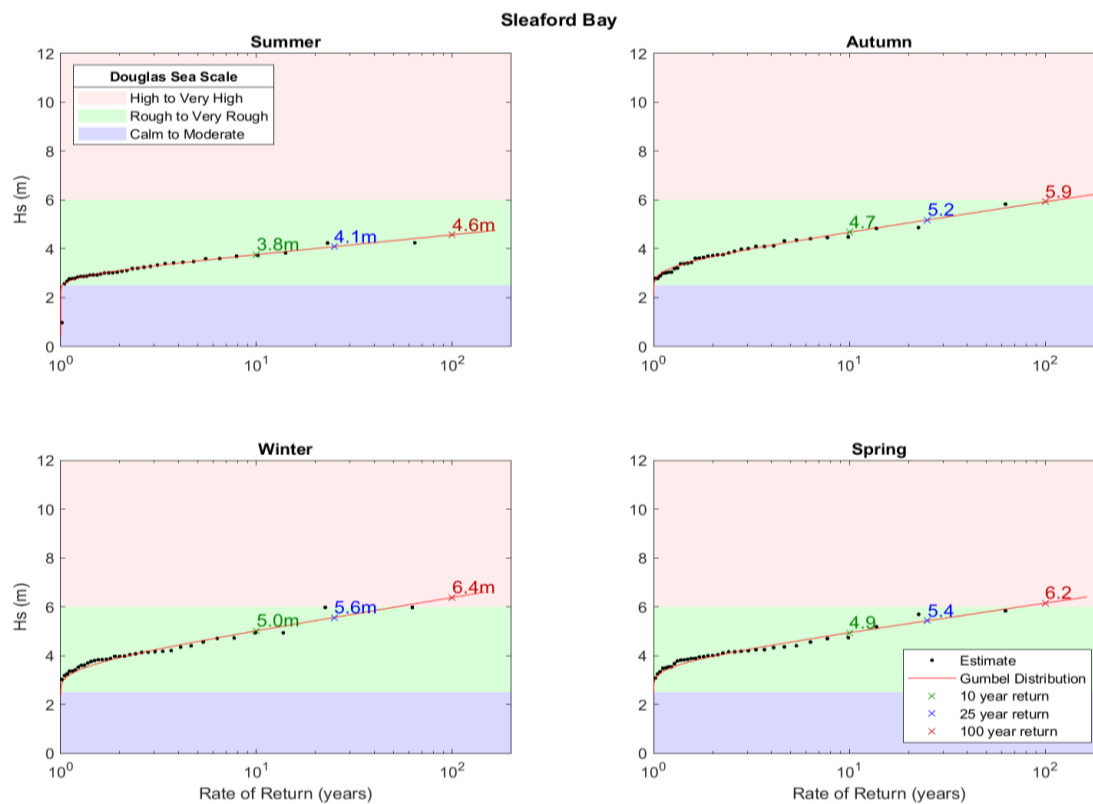
### 3.1.3 Waves: Seasonal analysis

The seasonal 100-year return heights for  $H_s$  indicate the biggest waves occur during winter and spring at both Sleaford Bay and Cape du Couedic (Table 1, Figure 10 and Figure 11). Again, the 100-year return heights were predicted to be much larger at the exposed Cape du Couedic site than at the more sheltered Sleaford Bay site.

**Table 1:** Summary of return-period heights for significant wave heights ( $H_s$ , in m) at Sleaford Bay and Cape du Couedic.

	Sleaford Bay			Cape du Couedic		
Season	10-year	25-year	100-year	10-year	25-year	100-year
Annual	5.4	5.9	6.7	9.7	10.4	11.4
Summer	3.8	4.1	4.6	6.8	7.4	8.4
Autumn	4.7	5.2	5.9	8.5	9.5	10.8
Winter	5.0	5.6	6.4	9.2	10.0	11.1
Spring	4.9	5.4	6.2	9.1	9.9	11.0

Looking at the mean direction of  $H_s$  (Figure 12 and Figure 13), there was more variability at the Cape du Couedic site, with waves tending to propagate more from the west during winter and spring and more from the south during summer and autumn. Waves were more consistent in direction at the Sleaford Bay site due to the limited exposure of the bay to swell from the west.

**Figure 10:** Return period (yrs) of extreme significant wave height ( $H_s$ ) events by season at Sleaford Bay.

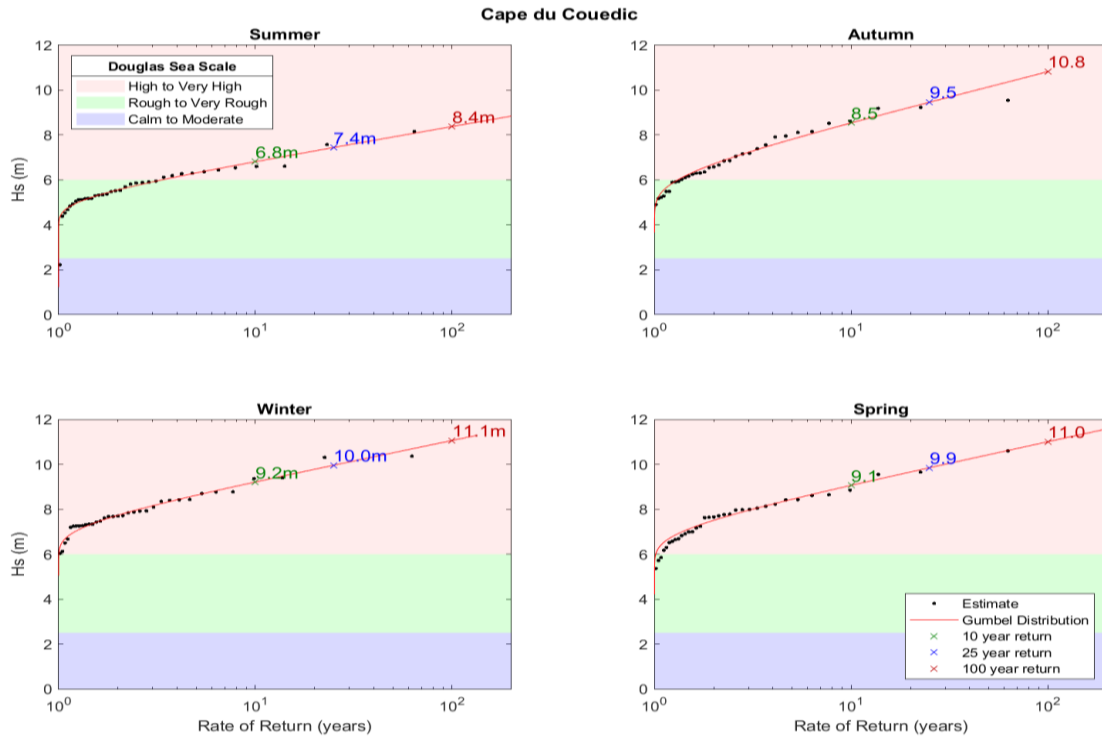


**Figure 11:** Return period (yrs) of extreme significant wave height (Hs) events by season at Cape du Couedic.

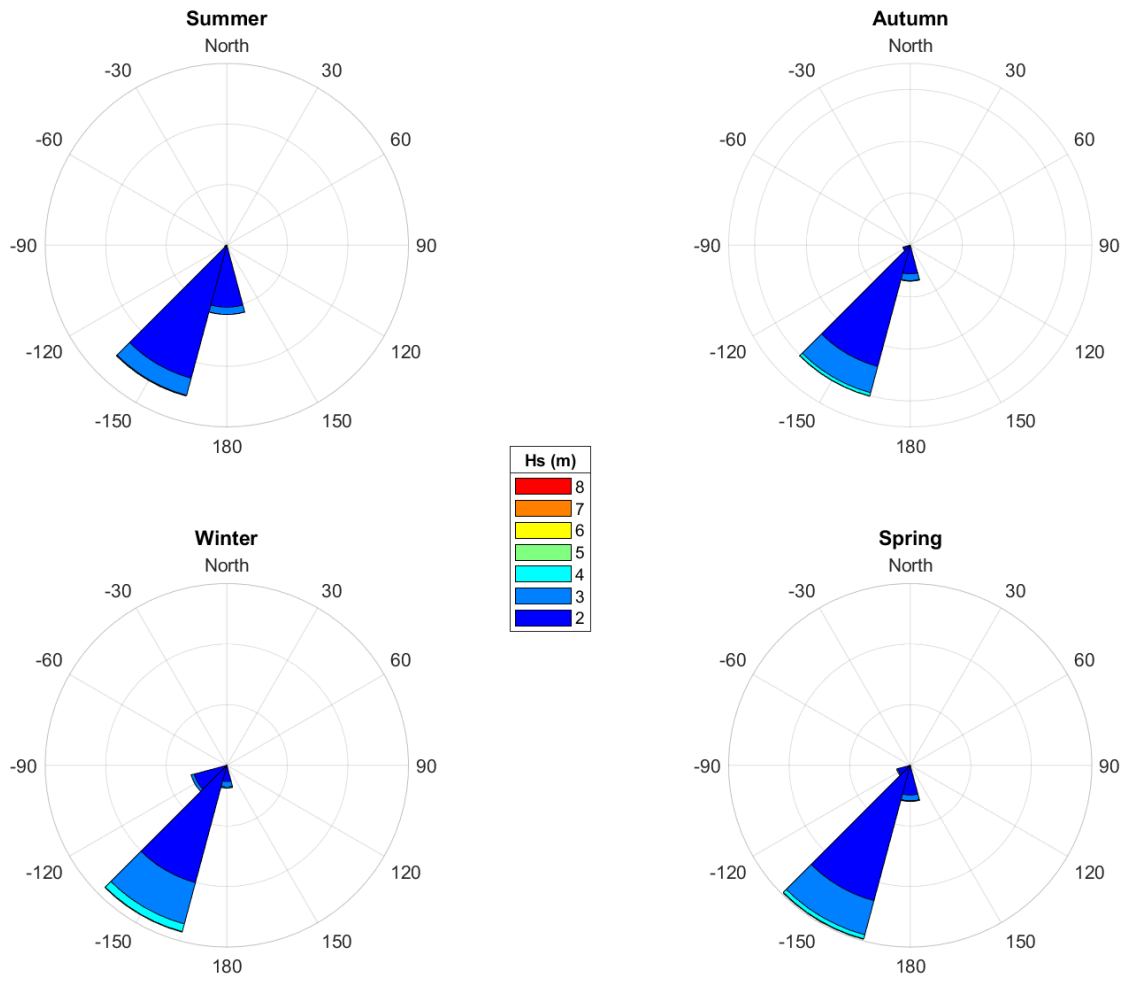


**Figure 12:** Sleaford Bay: seasonal significant wave height (Hs) as a function of wave direction.

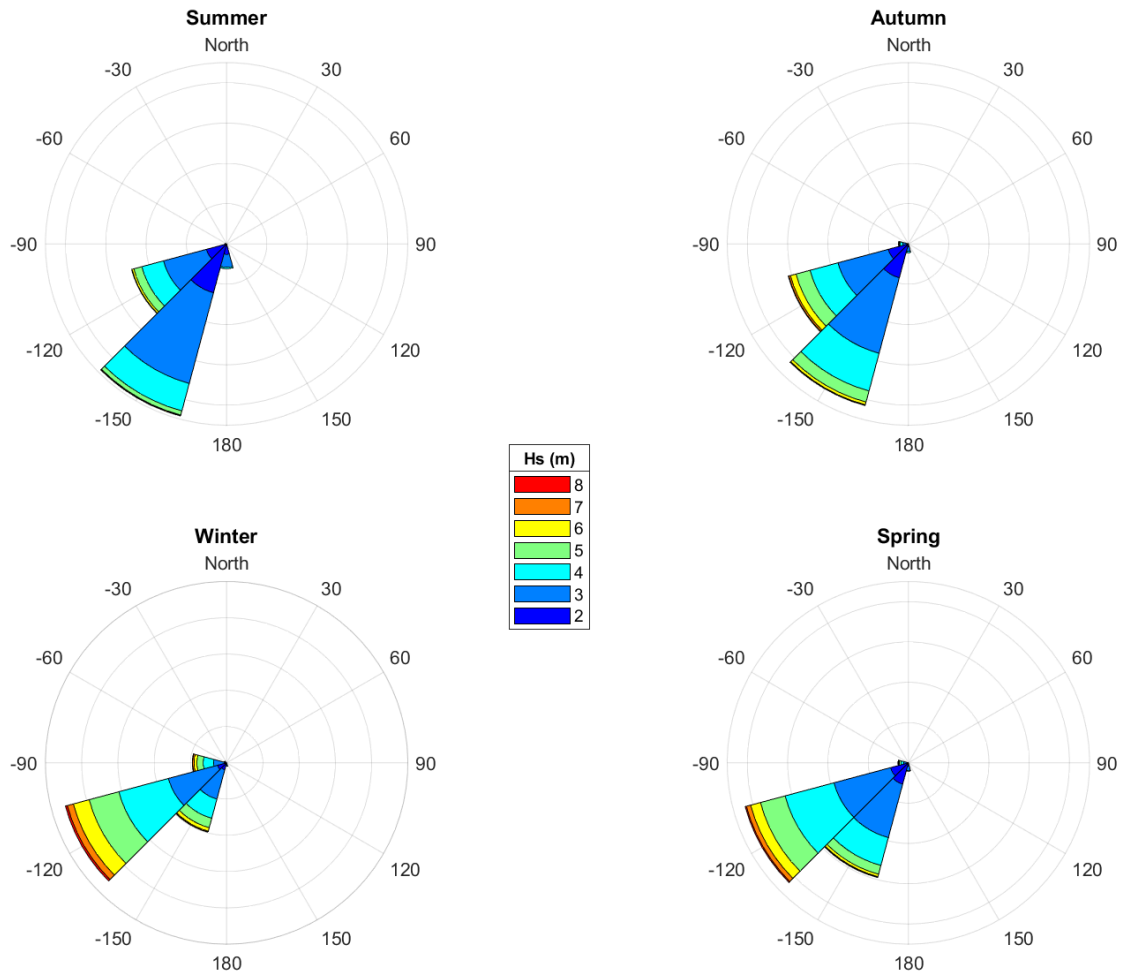


**Figure 13:** Cape du Couedic: seasonal significant wave height (Hs) as a function of wave direction.

Seasonal threshold analysis at Sleaford Bay supports this interpretation; the most days with favourable conditions occur in summer and the least number of favourable days occur in winter (Figure 14 and Figure 15).



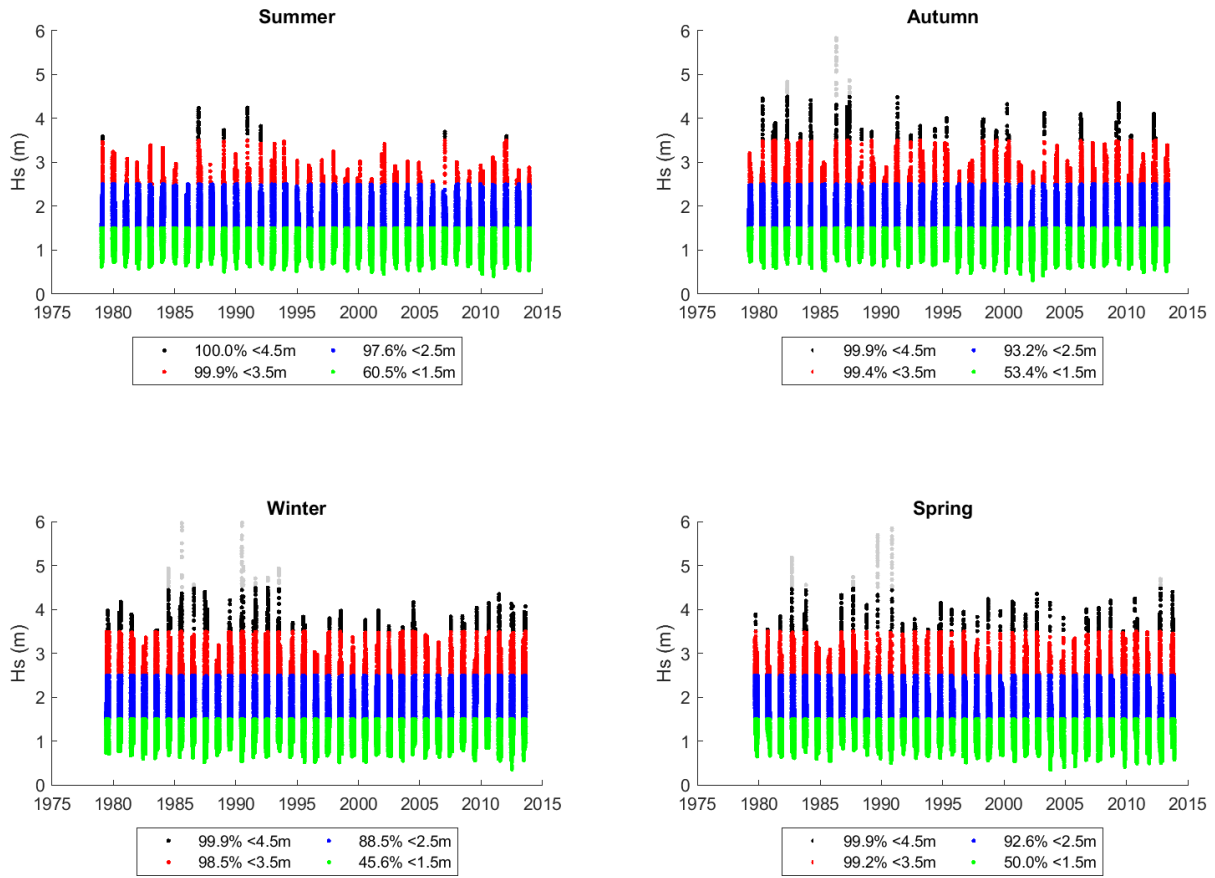
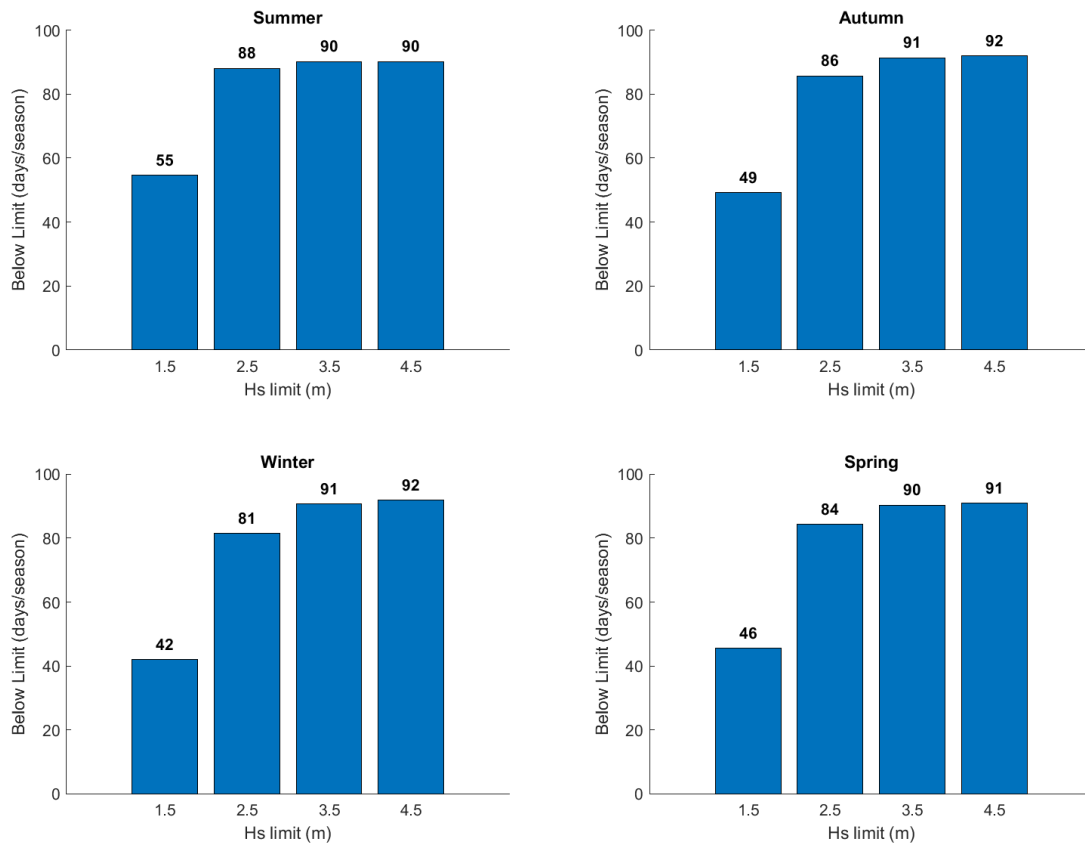


Figure 14: Seasonal threshold analysis of significant wave height (Hs) at Sleaford Bay.



**Figure 15:** Numbers of days with significant wave heights ( $H_s$ ) below threshold values, by season at Sleaford Bay.

### 3.1.4 Wind: Annual analysis

The 100-year return speeds for extreme wind events calculated for Sleaford Bay and Cape du Couedic are 83.8 km/h and 94.9 km/h respectively (Figure 16). Winds are consistently higher at the more exposed Cape du Couedic site, however the differences are not as pronounced as they are in the waves. Winds come out of the south-east and south-west more often and with greater intensity than other directions (Figure 17).

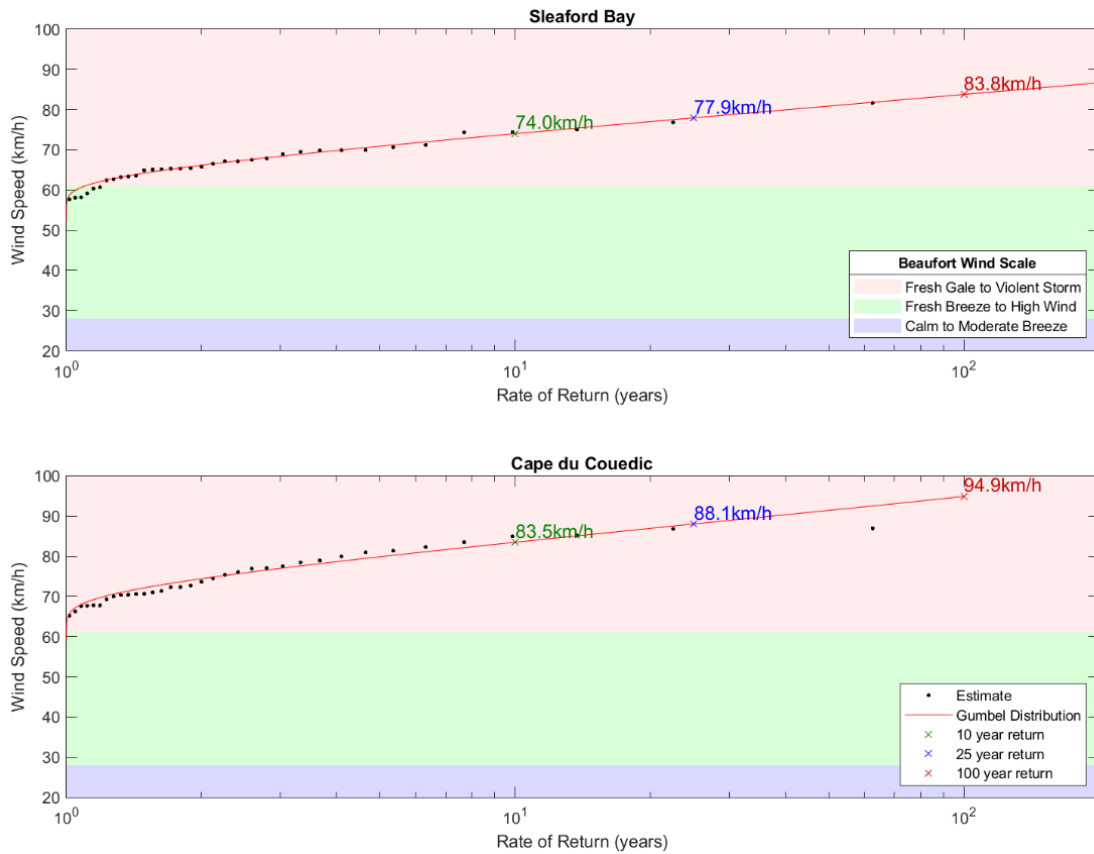


**Figure 16:** Return periods for extreme wind speeds ( $W$ ) at analysis sites

Threshold plots (Figure 18 and Figure 19) show that both sites have similar patterns of winds and that there are significant periods of time each year where winds are low enough to not adversely affect shipboard activities.

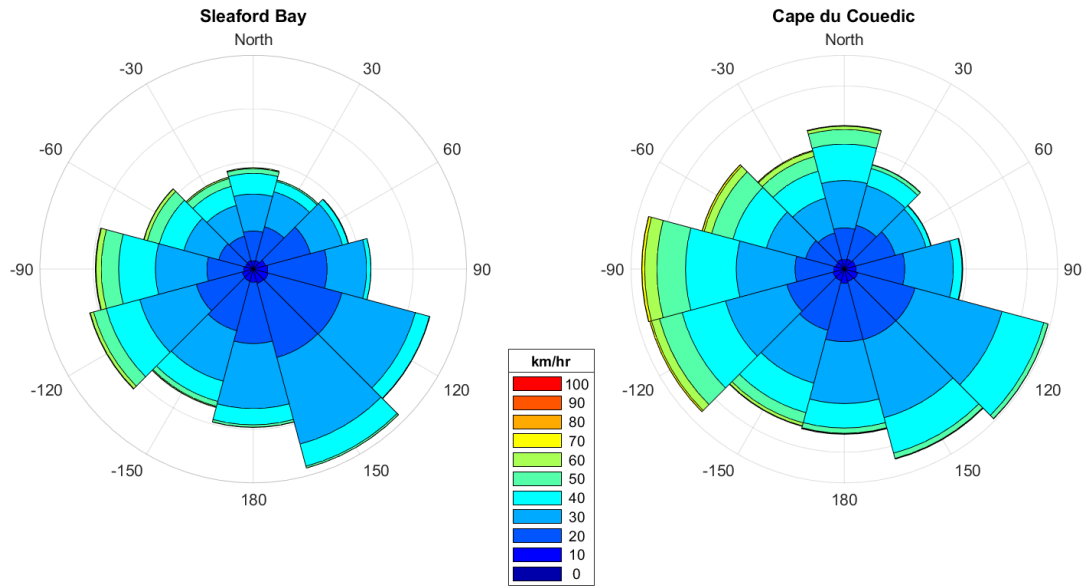


**Figure 17:** Wind speed (W) histograms as a function of direction for Sleaford Bay (left) and Cape du Couedic.

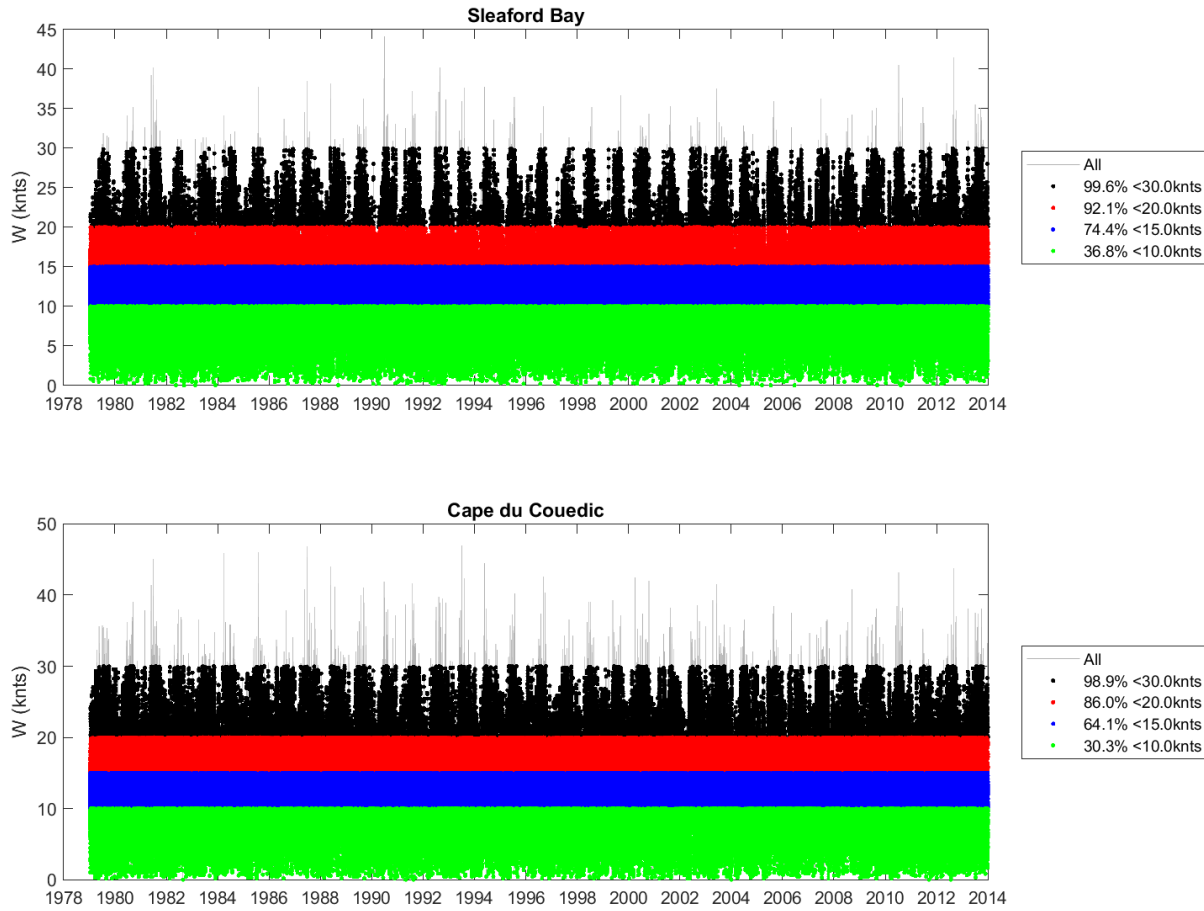


**Figure 18:** Frequency of wind speeds (W) below thresholds of 30, 20, 15 and 10 knots (55.6, 37.0, 27.8, and 18.5 km/h) for Sleaford Bay (top) and Cape du Couedic (bottom).

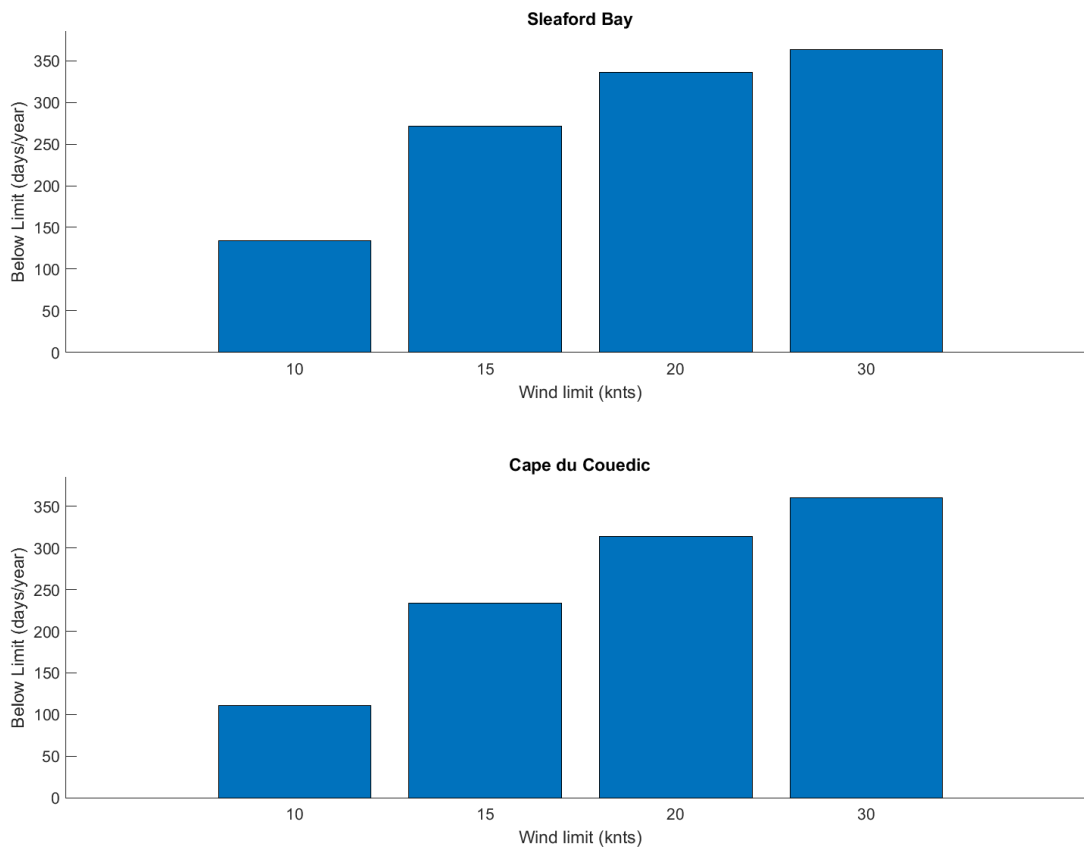


**Figure 19:** Number of days per year with wind speeds ( $W$ ) less than thresholds of 30, 20, 15 and 10 knots (55.6, 37.0, 27.8, and 18.5 km/h) for Sleaford Bay (top) and Cape du Couedic (bottom).

### 3.1.5 Wind: Seasonal analysis

Breaking down the winds by season at Sleaford Bay and Cape du Couedic, winter winds had the highest extreme values and summer winds had the lowest (Table 2). There was a difference between sites with spring winds being stronger than autumn winds at Sleaford Bay, and autumn winds being stronger than spring winds at Cape du Couedic (Figure 20 and Figure 21).

**Table 2:** Summary of return-period wind speeds ( $W$ ) for maximum winds (km/h) at Sleaford Bay and Cape du Couedic.

Season	Sleaford Bay			Cape du Couedic		
	10-year	25-year	100-year	10-year	25-year	100-year
Annual	74.0	77.9	83.8	83.5	88.1	94.9
Summer	54.9	58.7	64.3	62.7	66.8	72.9
Autumn	64.1	68.4	74.9	77.2	83.5	92.8
Winter	72.8	77.4	84.3	81.1	86.5	94.6
Spring	67.5	71.8	78.3	75.2	80.3	87.9

Wind directions show far more seasonal variability than wave directions. South-easterly winds clearly dominate during the summer at both sites (Figure 22 and Figure 23) and this was consistent with the strong upwelling events that occur along the southern shelf during this time of year (Kämpf et al. 2006, Middleton & Bye 2007). During the winter, winds more frequently come from the north-west. During the transition seasons of autumn and spring the winds are more variable relative to summer and winter.

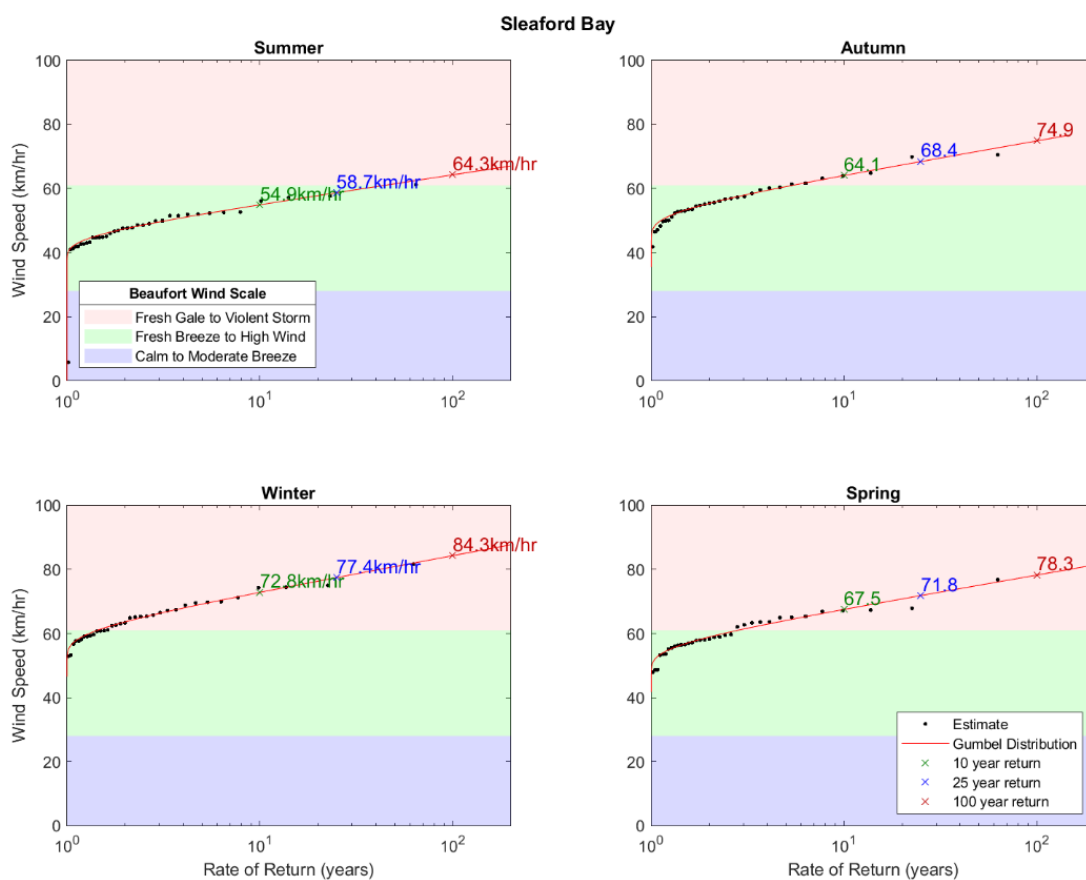


**Figure 20:** Return periods for extreme wind speeds ( $W$ ) by season at Sleaford Bay.

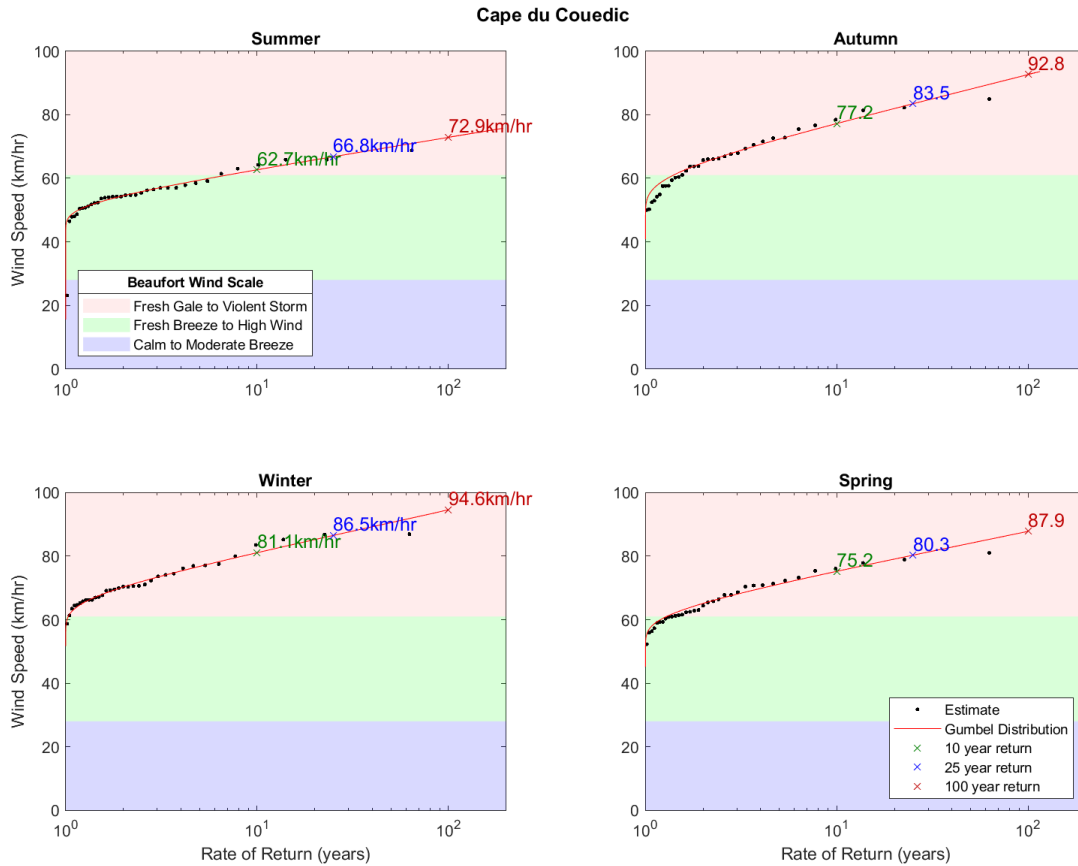


**Figure 21:** Return periods for extreme wind speeds (W) by season at Cape du Couedic.



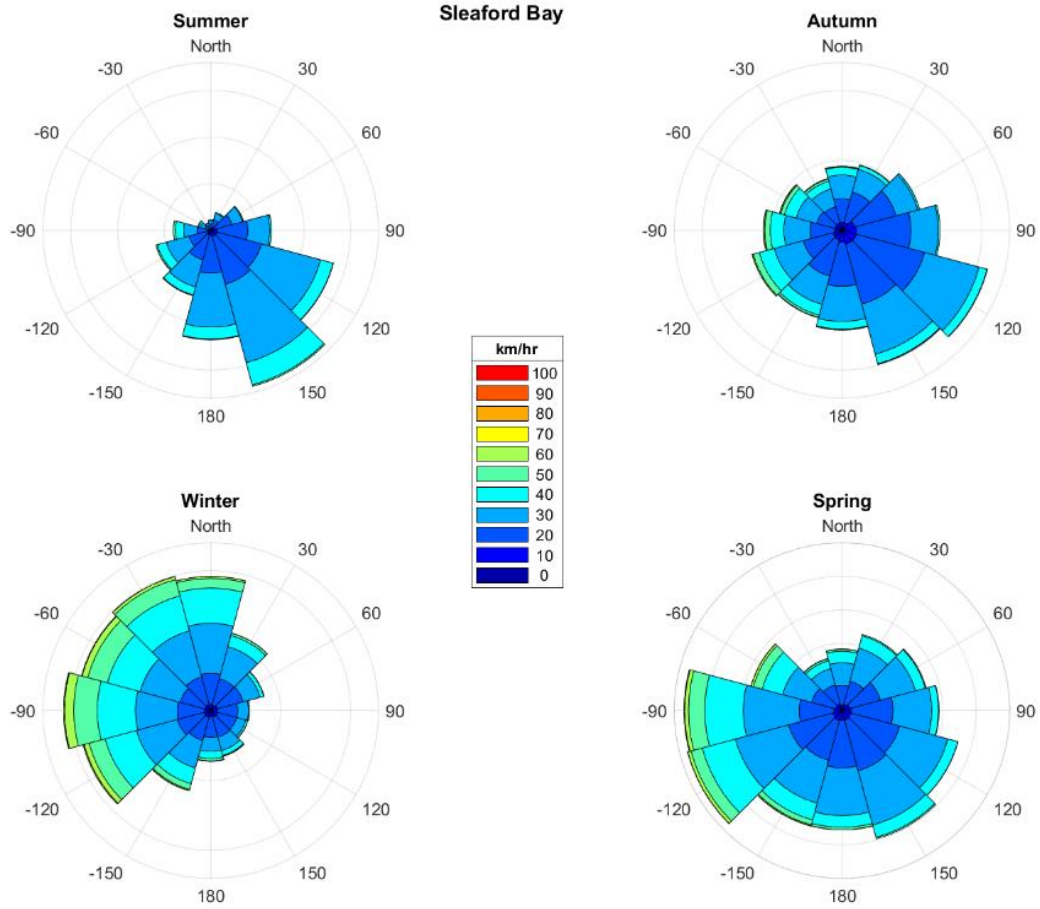


**Figure 22:** Wind speed (W) as a function of wind direction at Sleaford Bay.

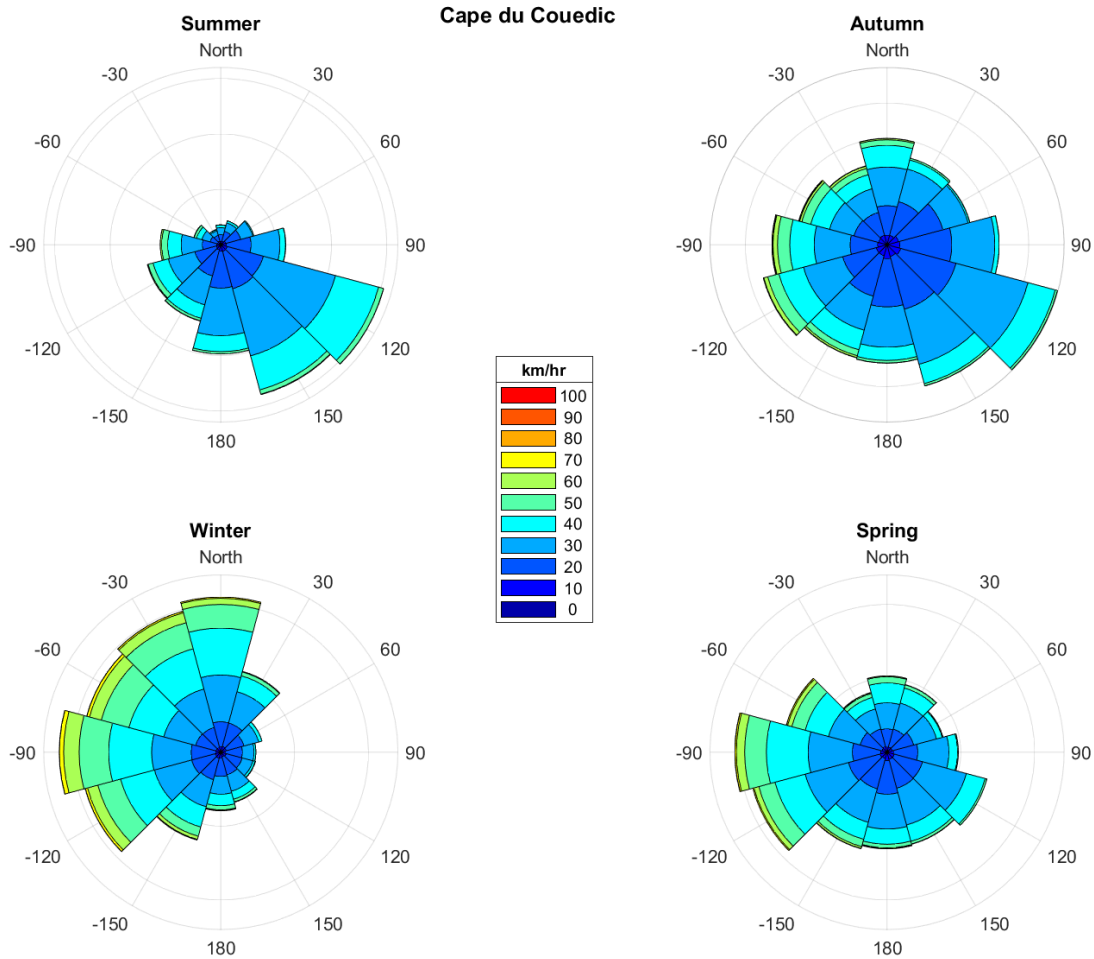


**Figure 23:** Wind speed ( $W$ ) as a function of wind direction at Cape du Couedic.

Looking at seasonal thresholds at Sleaford Bay, for most years  $W$  will exceed the maximum threshold (30 knots) for some days during the winter, which also has the fewest days with  $W$  below the lowest threshold (10 knots) (Figure 24 and Figure 25). On average autumn has the most days with winds below the lowest threshold.

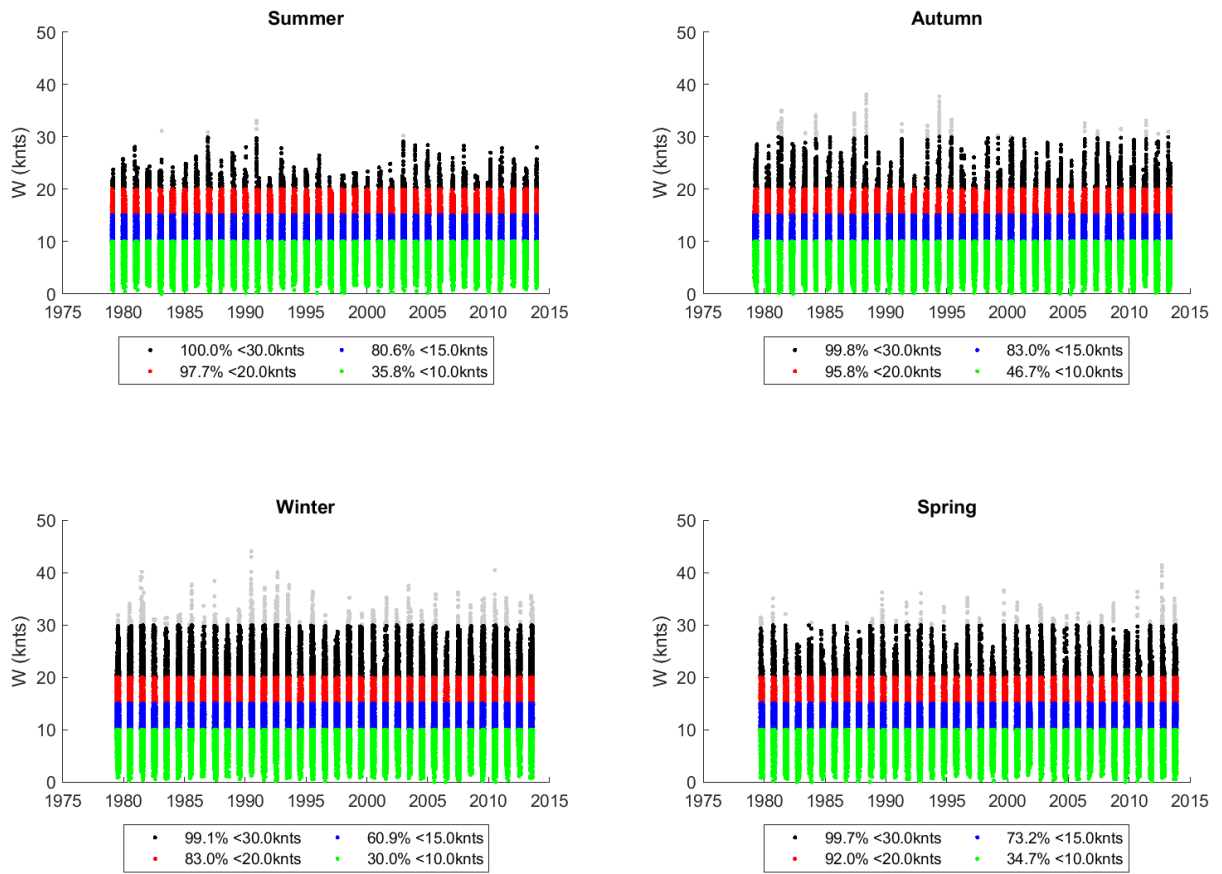
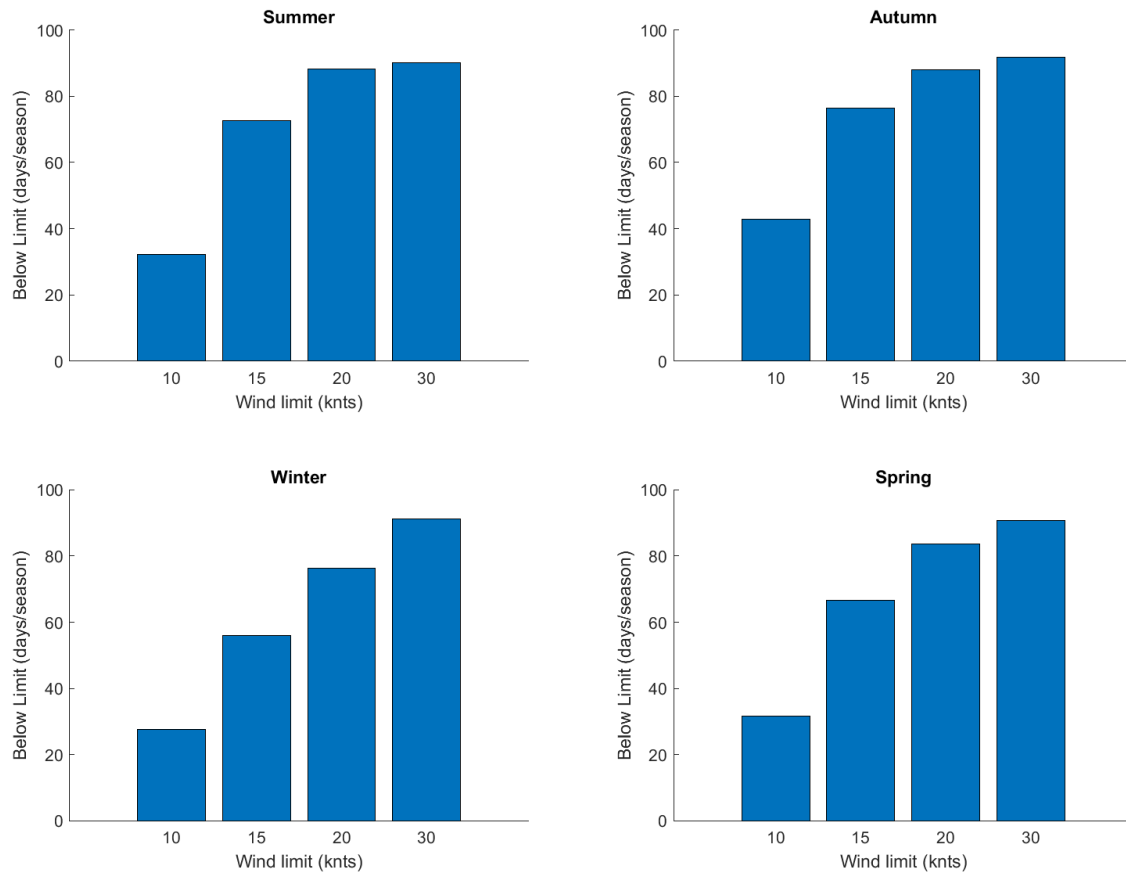


Figure 24: Seasonal Threshold analysis of wind speed (W) at Sleaford Bay.



**Figure 25:** Number of days with winds below threshold values, by season at Sleaford Bay (total days for summer=90, autumn=92, winter=92, and spring=91).

### 3.1.6 Wave height (Hs) versus wave period (Tp)

For engineering purposes, it is useful to characterise the waves by combined wave-height and period properties. An analysis of the Hs and Tp values for all waves at the Sleaford Bay site indicated that the highest percentage of waves were between 1.0 and 2.0 m with Tp values between 12 and 16 sec. (Table 3). A scatter plot shows visually the extent of the variability in wave characteristics over the 30+ years of model output (Figure 26).

**Table 3:** Distribution of significant wave height (Hs) versus peak wave period (Tp) at Sleaford Bay: indicated are the percentage of waves with characteristics lying within 0.5 m x 2 s bins.

Hs (m)	Tp (s)													Totals
	2-4	4-6	6-8	8-10	10-12	12-14	14-16	16-18	18-20	20-22	22-24	24-26	26-28	
0.0-0.5				0.00	0.04	0.02	0.00	0.00						0.07
0.5-1.0	0.00	0.07	0.42	1.01	2.72	5.73	3.17	0.44	0.07	0.00	0.00			13.64
1.0-1.5	0.00	0.07	1.04	2.52	7.07	13.73	12.24	2.58	0.39	0.05	0.01	0.00		39.70
1.5-2.0		0.00	0.22	1.25	3.86	9.05	10.62	3.02	0.43	0.08	0.02	0.00	0.00	28.55
2.0-2.5	0.00		0.00	0.21	0.94	2.98	5.48	2.00	0.33	0.06	0.02	0.01	0.00	12.03
2.5-3.0				0.02	0.20	0.63	2.00	1.15	0.23	0.02	0.01	0.00	0.00	4.26
3.0-3.5				0.00	0.03	0.12	0.54	0.50	0.10	0.01	0.00		0.00	1.29
3.5-4.0					0.00	0.02	0.11	0.20	0.03	0.00	0.00			0.36
4.0-4.5						0.00	0.01	0.05	0.01	0.00				0.07
4.5-5.0							0.00	0.00	0.01					0.02
5.0-5.5							0.00	0.00	0.00	0.00				0.01
5.5-6.0									0.00	0.00				0.00
<b>Totals</b>	0.00	0.14	1.69	5.01	14.86	32.28	34.18	9.93	1.61	0.22	0.06	0.01	0.00	100.00

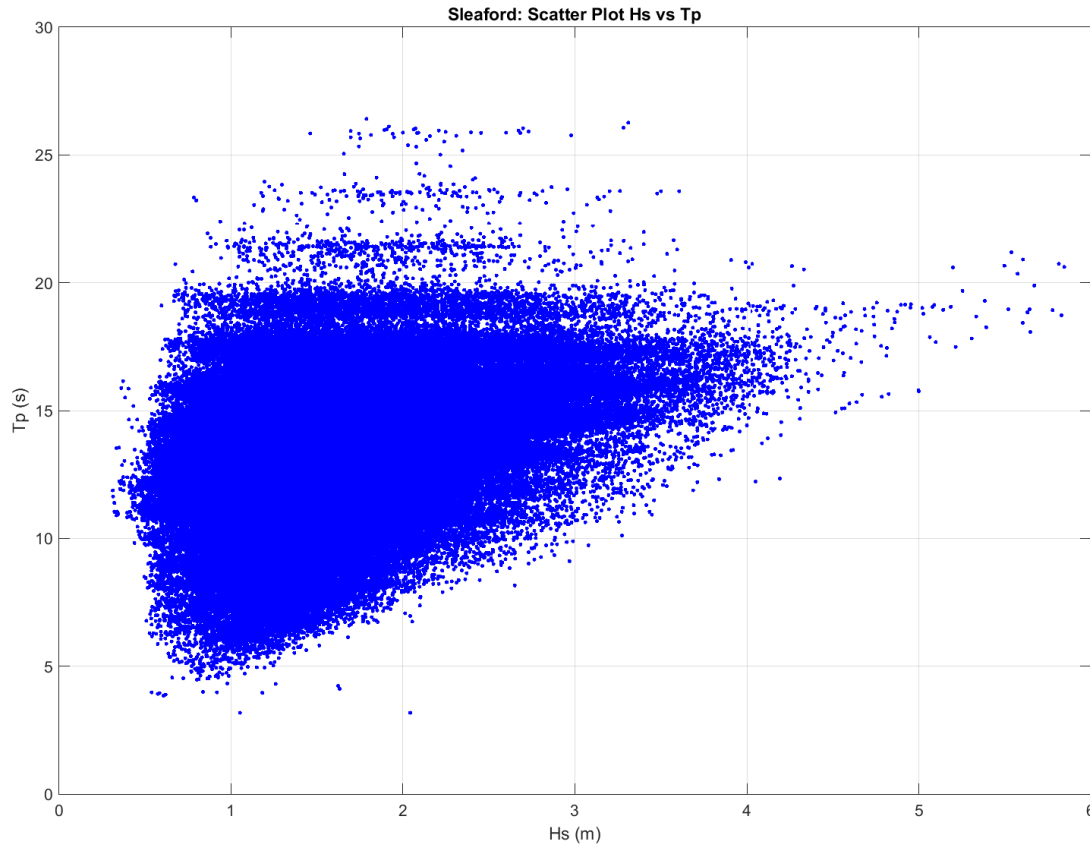


**Figure 26:** Scatter plot of modelled significant wave height ( $H_s$ ) against peak wave period ( $T_p$ ) at Sleaford Bay.

### 3.1.7 Current Analysis

The final model analysis was an investigation of current patterns within Sleaford Bay (Figure 27). In the absence of long-term observations, Vertically averaged velocity ( $V_{bar}$ ) at the Sleaford Bay site was extracted from three years of model data from the TGM, the eSA-Marine 1.5 km, two gulfs model previously used for tracer studies in the gulfs (Rogers et al. 2020). Three years is too short a time-series for accurate return-period analysis, but some general comments on the current patterns can be made.

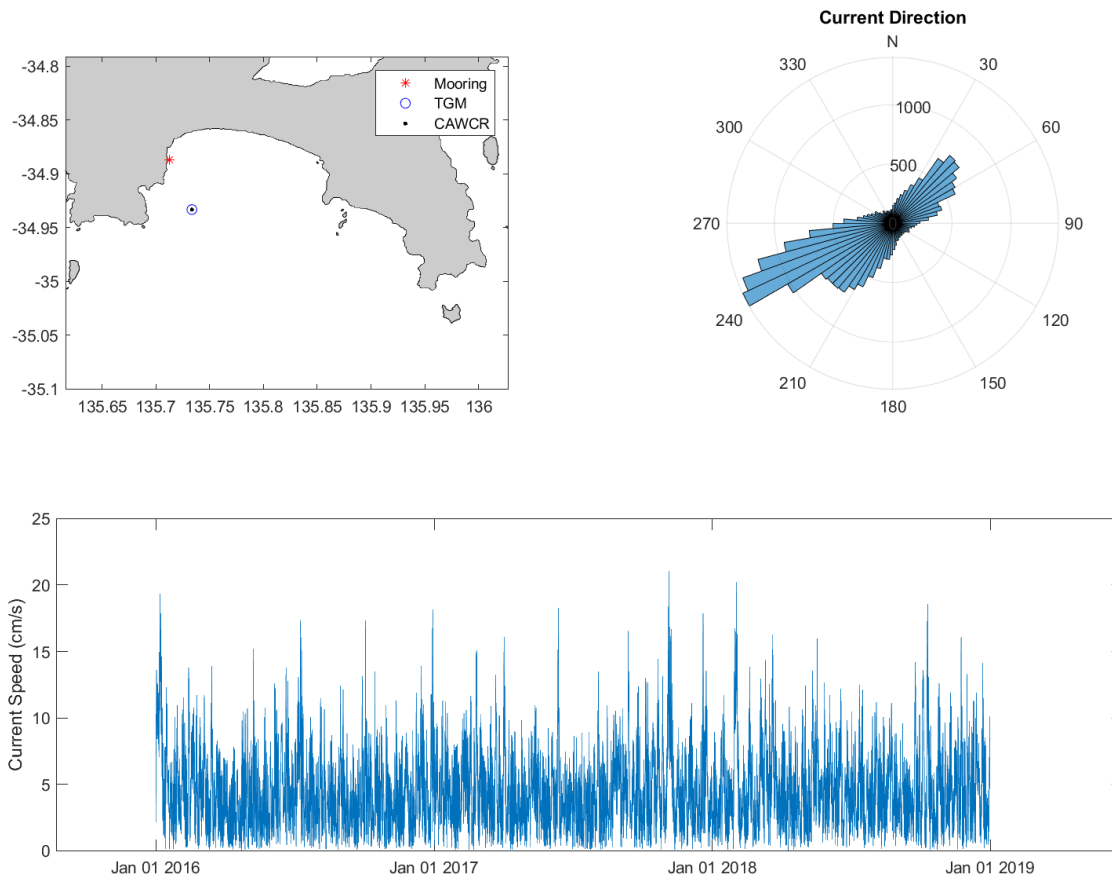


**Figure 27:** Location, speed and direction of modelled ocean currents at Sleaford Bay. The map indicates the location of the mooring site relative to the CAWCR and TGM modelled grid-points.

Currents occur most frequently along the north-east/south-west axis, with speeds rarely exceeding 15 cm/s. The weaker tidal currents generally follow the same directions, within a tighter range and below 5 cm/s (Figure 28).

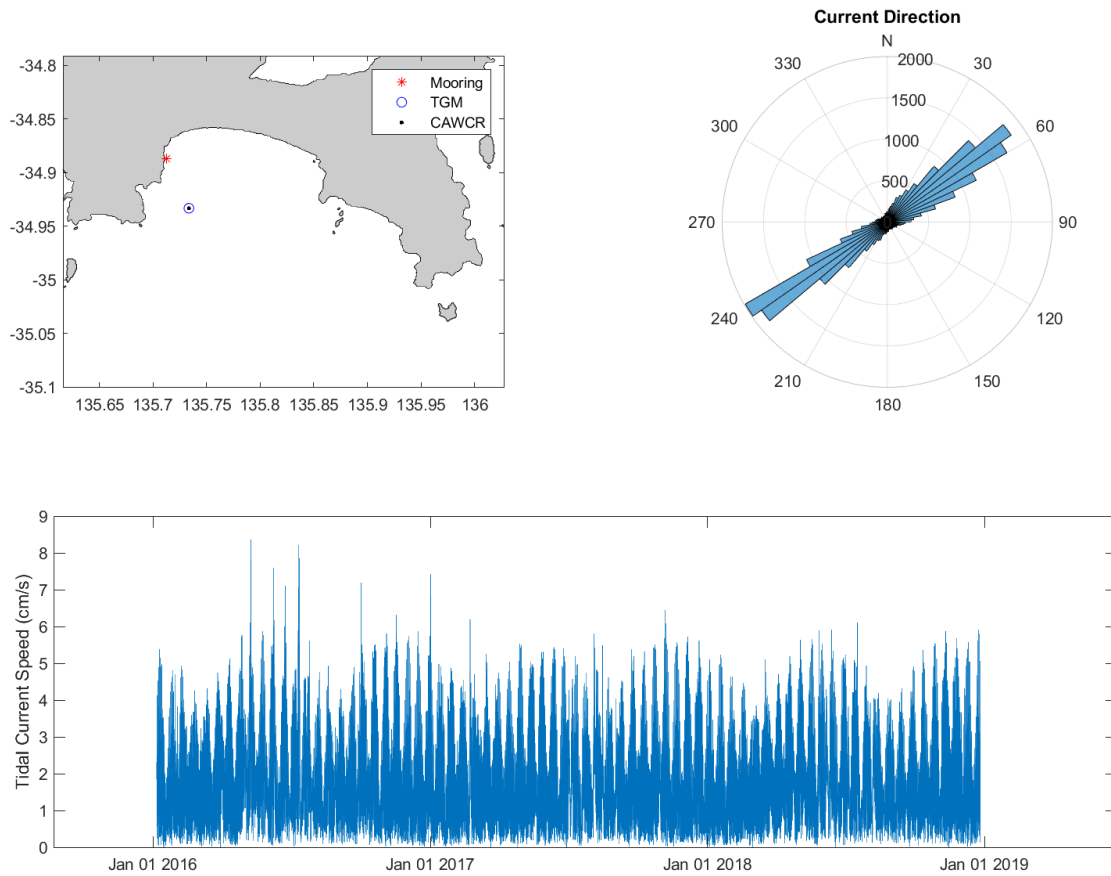


**Figure 28:** Location, speed and direction of modelled tidal currents at Sleaford Bay. The map indicates the location of the mooring site relative to the CAWCR and TGM modelled grid-points.

The model has sufficient resolution to map the general circulation within the bay, averaging across all three years and separating into four seasons (Figure 29),  $\bar{V}$  was dominated by a persistent counter-clockwise eddy. The offshore flow intensified from the west during winter and spring, however the bay remained sheltered and the seasonally-averaged velocity generally remained below the 5 cm/s level.



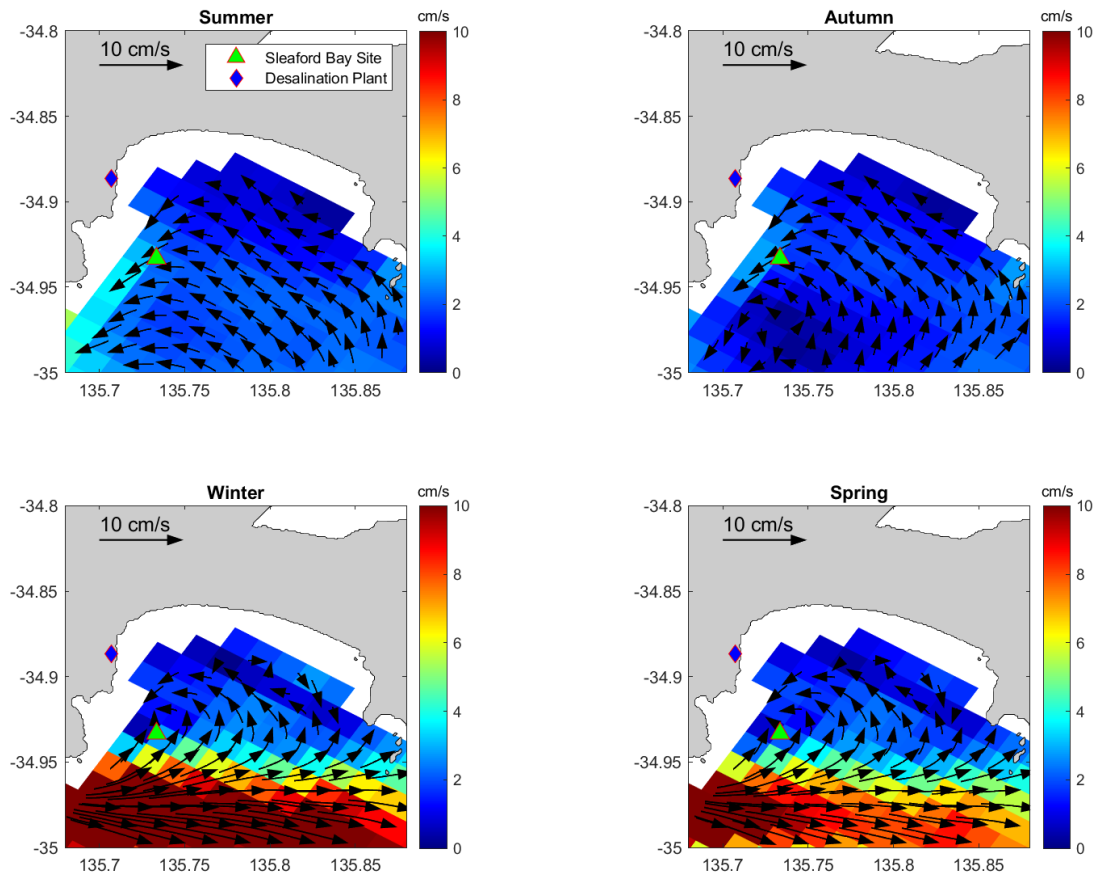


**Figure 29:** Seasonal current patterns within Sleaford Bay based on averages for 2016-2018.

## 3.2 *In situ* mooring observations

### 3.2.1 Waves

The time-series of wave height ( $H_s$  and  $H_{max}$ ) and wave period ( $T_p$ ) measured by the moored ADCP is shown in Figure 30. Significant wave heights ( $H_s$ ) ranged between 0.5 and 2.5 m and maximum wave heights ( $H_{max}$ ) reached 4.5 m (Figure 29). The median ratio of  $H_{max}$  to  $H_s$  was 1.5 (range 1.2 to 2.0 m), which, for a relatively short time-series, is consistent with the suggested scaling of 1.6 (see Appendix). Peak wave period ( $T_p$ ) ranged between 5 and 17 s, consistent with periods expected for locally generated wind-waves and swell, respectively. The average directional wave power spectrum showed the maximum wave energy ( $m^2/Hz$ ) was associated with swell, with  $T_p$  greater than 10 s, arriving from the south-east (Figure 31). The narrow swell direction window of  $135-155^\circ$  indicated swells received at the mooring site were strongly refracted towards the coastline. For  $T_p$  values less than 10 s, the directional spectrum showed more variability, with locally generated wind-waves still predominantly coming from the east and south.

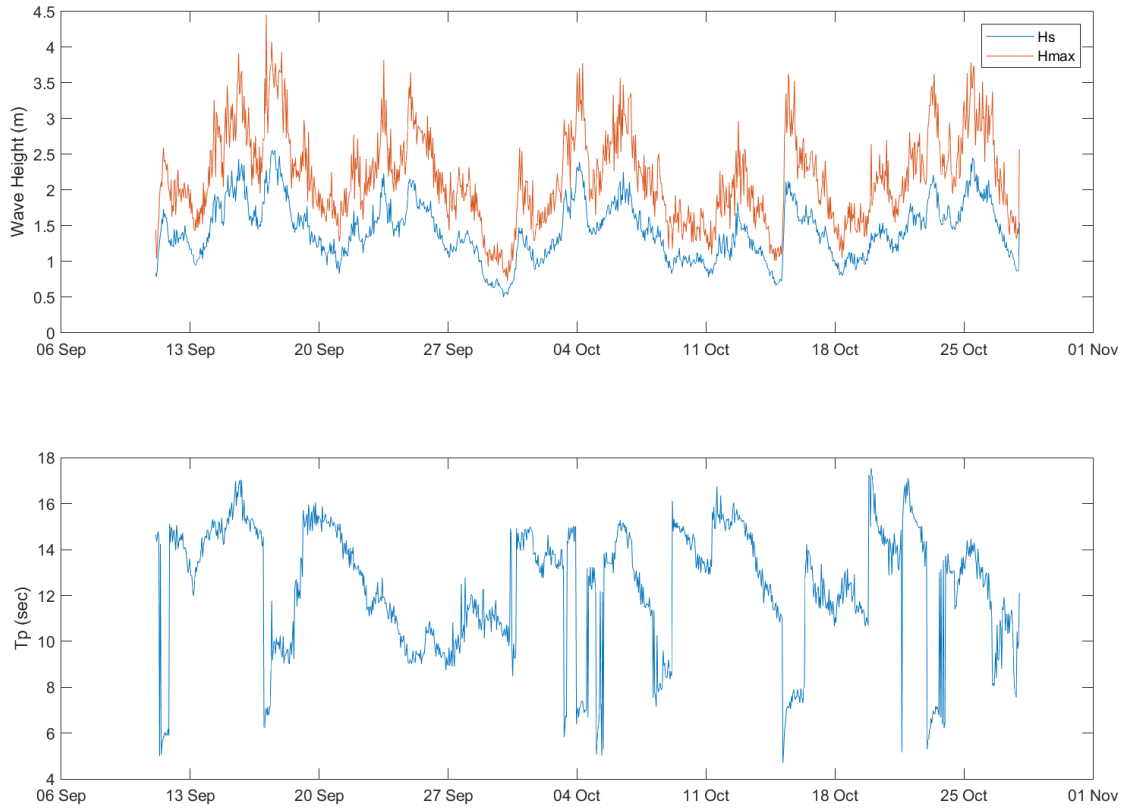


**Figure 30:** Observations of significant wave height ( $H_s$ ) and peak period ( $T_p$ ) measured by the moored ADCP.

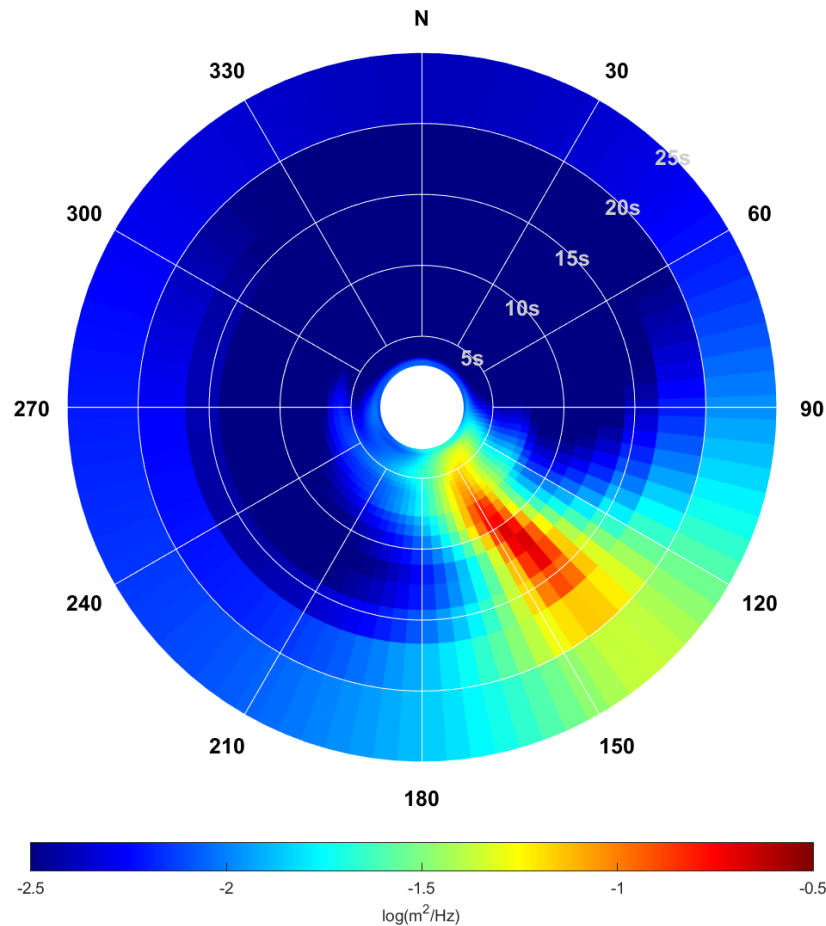


**Figure 31:** Average directional wave spectrum measured by the Acoustic Doppler Current Profiler (ADCP) in Sleaford Bay.

### 3.2.2 Currents

The time-series of depth-averaged current speeds and directions measured by the moored ADCP are shown in Figure 32. The currents were strongly aligned along isobaths on a north-south axis. Current speeds were generally below 6 cm/s, however maximum current speeds of up to 20 cm/s were observed, lasting up to several days. Removal of the tidal currents using a low-pass digital filter (Thompson 1983) showed the dominant currents of up to 12 cm/s were non-tidal and followed the same north-south axis with less directional variability (Figure 33). Hence, for the observed time-series, tidal currents were weaker and expected to be below 8 cm/s.

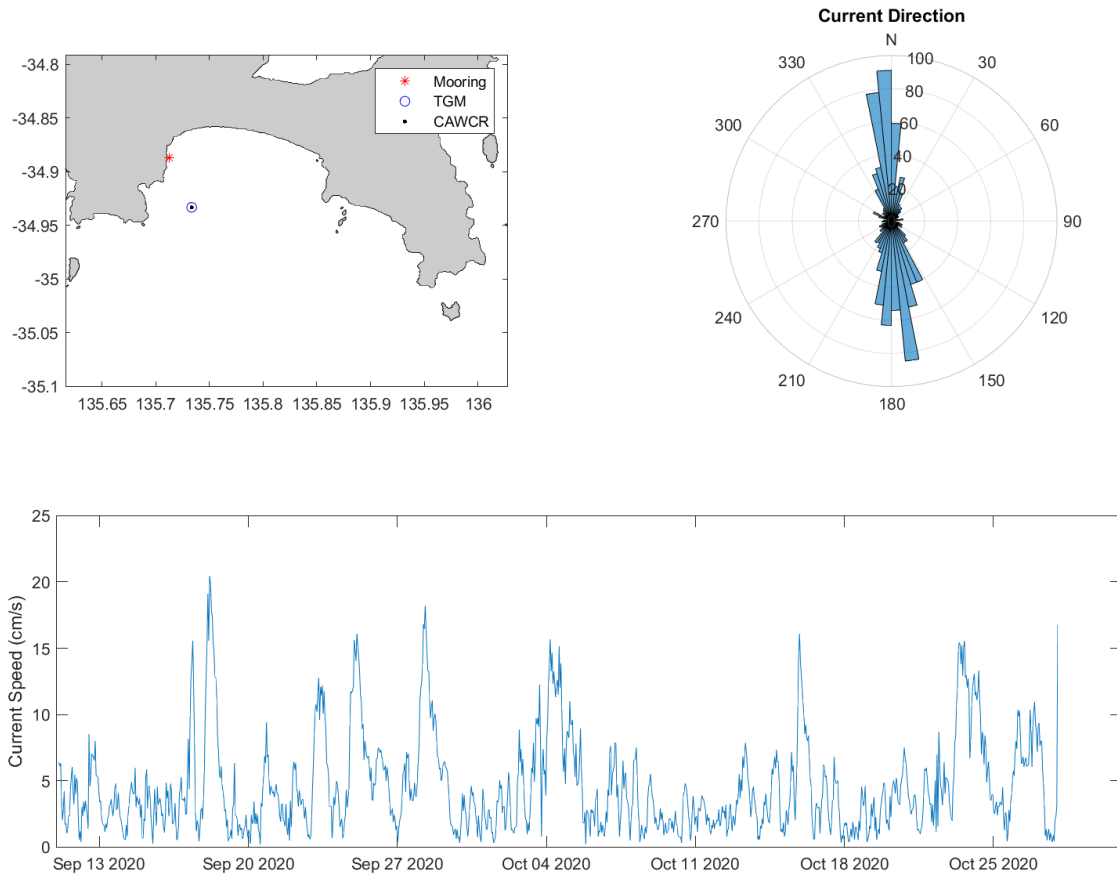


**Figure 32:** Depth-averaged current speeds and directions measured by the Acoustic Doppler Current Profiler (ADCP) in Sleaford Bay. The map indicates the location of the mooring site relative to the CAWCR and TGM modelled grid-points.

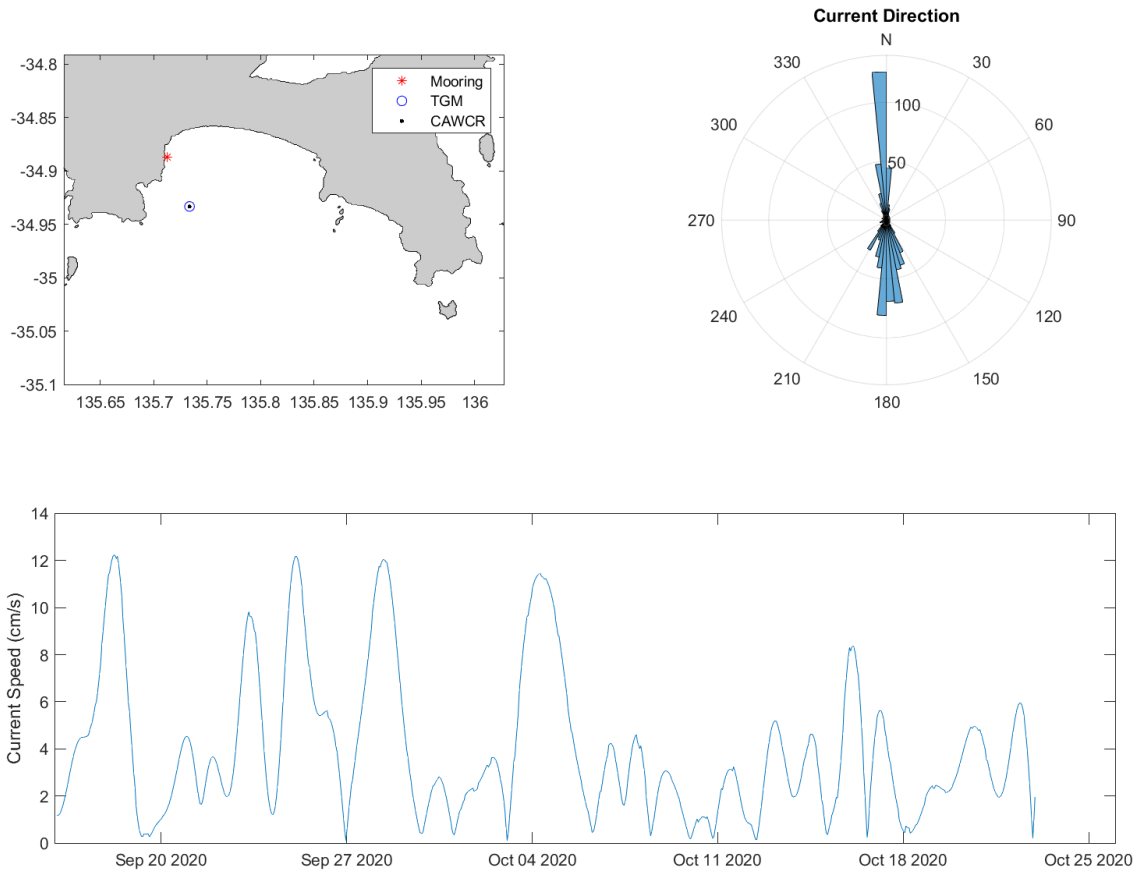


**Figure 33:** Tide filtered depth-averaged current speeds and directions measured by the Acoustic Doppler Current Profiler (ADCP) in Sleaford Bay. The map indicates the location of the mooring site relative to the CAWCR and TGM modelled grid-points

## 4 CONCLUSIONS

Information is presented on the sea conditions expected at the location of a proposed desalination plant site in Sleaford Bay, South Australia. To produce this analysis, long time series of ocean measurements necessary for characterizing the sea-state and the probability of extreme events were obtained from global and regional ocean models. To provide verification of the model results and account for model limitations, direct observations of waves and currents were taken in September and October 2020.

Model results for winds indicated wind speeds in Sleaford Bay are generally below 18.5 km/h (15 knots) for most of the year. However, extreme event analysis shows strong, sustained winds are possible with a 100-year return speed of 83 km/h (45 knots). Wind patterns showed a strong seasonality, with south-easterlies dominating through the summer months and north-westerlies during the winter.

For waves, comparison of the Centre for Australian Weather and Climate Research (CAWCR) wave hindcasts and extensions reanalysis model (Durrant et al. 2014) with wave data from the Bureau of Meteorology's Cape du Couedic WaveRider Buoy suggests that the 30-year model predictions could provide a suitable time-series for analysing wave conditions around the South Australian Coast. Compared with Cape du Couedic, Sleaford Bay is relatively well sheltered from the harsh wave conditions experienced further off-shore, however a return period analysis suggests that significant waves heights ( $H_s$ ) in excess of 3 m are not uncommon with a 100-year return height of nearly 6.7 m, and with the worst conditions found during the winter. Wave periods associated with the swell are relatively long, and the 100-year return period for  $T_p$  is 28.9 s. Threshold analysis suggest that wave events with  $H_s$  over 3.5 m can be expected to occur at least once each year. These results are supported by direct wave observations made during September and October, 2020. Observed significant wave heights remained below 2.5 m with a maximum  $T_p$  of 17 s. Compared to the model results, observed wave directions were predominantly from the south-east as a result of the deployment site being located much closer to the coast than the site used for model predictions, and subsequent wave refraction due to interactions with local bathymetry.

Model results indicate the ocean currents within Sleaford Bay are dominated by a counter-clockwise eddy, these currents are generally quite weak and of the same order of magnitude as the tidal currents – approximately 5 cm/s. Maximum currents at the Sleaford Bay site, near the proposed desalination plant, were rarely found to exceed 20 cm/s. These results are consistent

with the *in situ* measures of current speed, with the observed depth-averaged current strongly orientated along isobaths with a north–south axis.

Overall, the findings in this report provide for a detailed characterization and assessment of the wind and sea conditions that will be experienced in Sleaford Bay and have the potential to influence future desalination plant development and activities. Due to the closeness of the proposed intake/outfall site to the shoreline, additional observations of waves and currents during energetic winter periods would aid in understanding and validating the extreme values predicted for waves and currents at the proposed site.

## 5 REFERENCES

Durrant, T., Greenslade, D., Hemer, M., Trenham, C., (2014). *A Global Wave Hindcast focussed on the Central and South Pacific*. CAWCR Technical Report 070.

Gringorten, I.I., (1963). *A Plotting Rule for Extreme Probability Paper*. J. Geophys. Res., Vol. 68, No. 3, pp. 813-814.

James, C. and Doubell, M.J., (2020). Long-term analysis of the sea-state in the Great Australian Bight, The University of Adelaide and SARDI (Aquatic Sciences), FRDC Project No. 2018/210.

Kämpf, J., (2010). On preconditioning of coastal upwelling in the eastern Great Australian Bight. J. Geophys. Res. Oceans 115, C12071. <https://doi.org/10.1029/2010JC006294>

Laloyaux, P., de Boisseson, E., Balmaseda, M., Bidlot, J.R., Broennimann, S., Buizza, R., Dalhgren, P., Dee, D., Haimberger, L., Hersbach, H. and Kosaka, Y., (2018). CERA-20C: A coupled reanalysis of the Twentieth Century. Journal of Advances in Modeling Earth Systems, 10(5), pp.1172-1195.

Middleton, J.F., Bye, J.A.T., (2007). A review of the shelf-slope circulation along Australia's southern shelves: Cape Leeuwin to Portland. Prog. Oceanogr. 75, 1–41.

Rogers, T.A., Redondo-Rodriguez, A., Fowler, A.J., Doubell, M., Drew, M.J., Steer, M.A., Matthews, D., James, C., Gillanders, B.M., (2020). Using a biophysical model to investigate connectivity between spawning grounds and nursery areas of King George whiting (*Sillaginodes punctatus*: Perciformes) in South Australia's gulfs, Fish. Oceanogr., 1-18. <https://doi.org/10.1111/fog.12502>

Sverdrup, H.U. and Munk, W.H. (1947). *Wind, sea and swell: Theory of relations for forecasting* (No. 303). US Hydrographic Office, Washington DC.

Thompson, R., (1983). Low-pass filters to suppress inertial and tidal frequencies. J. Phys. Oceanogr., 13: 1077-1083.



## 6 APPENDIX

For engineering purposes, the value of the maximum wave height ( $H_{max}$ ) is often required. One of the few long-term reanalysis wave models to include both  $H_{max}$  and  $H_s$  is the CERA-20C (Laloyaux et al. 2018) model available from the European Centre for Medium Range Weather Forecasts (ECMWF). The global grid is too coarse to represent Sleaford Bay, however, we have collected model output from 1970-2010 for a recent report on the nearby Great Australian Bight (GAB) sea-state (James and Doubell, 2020). This, in conjunction with the observational data from the WaveRider Buoy at Cape du Couedic, can be used to investigate the local relationship between  $H_{max}$  and  $H_s$ .

Globally the relationship between  $H_s$  and  $H_{max}$  can be quite complex,  $H_{max}$  is often transient and sub-grid scale and may depend on the interaction of waves from different directions. In South Australia, however, the consistent swell direction means that we can make a linear estimate of  $H_{max}$  based on  $H_s$ . At both the GAB site (130.8E 34.9S) and Cape du Couedic,  $H_{max}$  and  $H_s$  are highly correlated (Figure 34). Regression through the origin gives a ratio ( $R = H_{max}/H_s$ ) of 1.5 and 1.65 for the GAB and Cape du Couedic, respectively.

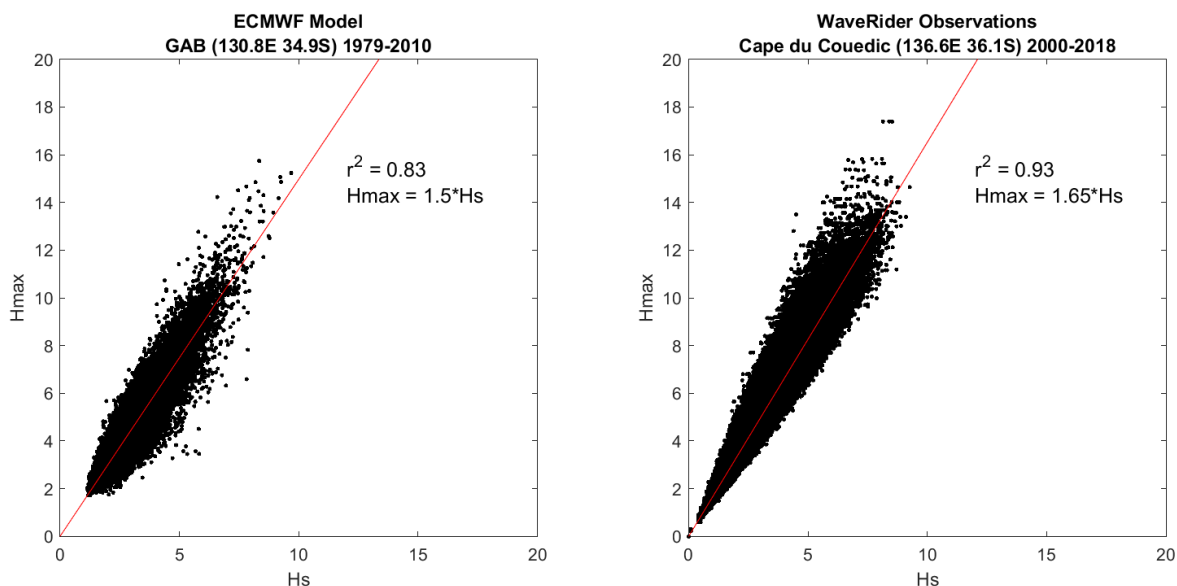


**Figure 34:** Correlation and linear regression through the origin of maximum wave height ( $H_{max}$ ) as a function of significant wave height ( $H_s$ ) at a site in the Great Australian Bight (GAB) (left) and the Cape du Couedic WaveRider mooring.

To examine the sensitivity of  $R$  to  $H_s$  we can compute  $R$  for every time step in both time-series and then average the ratio into 0.5 m bins of  $H_s$  from 0 to 10m in (Figure 35). Histograms of  $R$  indicate roughly normal distributions around the means of 1.52 and 1.67. The mean values of  $R$  remain relatively flat along the range of observed  $H_s$  values which suggests that a constant conversion value can be used for all  $H_s$ . The average of the four estimates, 1.50, 1.52, 1.65, and 1.67 is 1.59 and suggests a rounded value of 1.6 would be an appropriate scaling for this region.

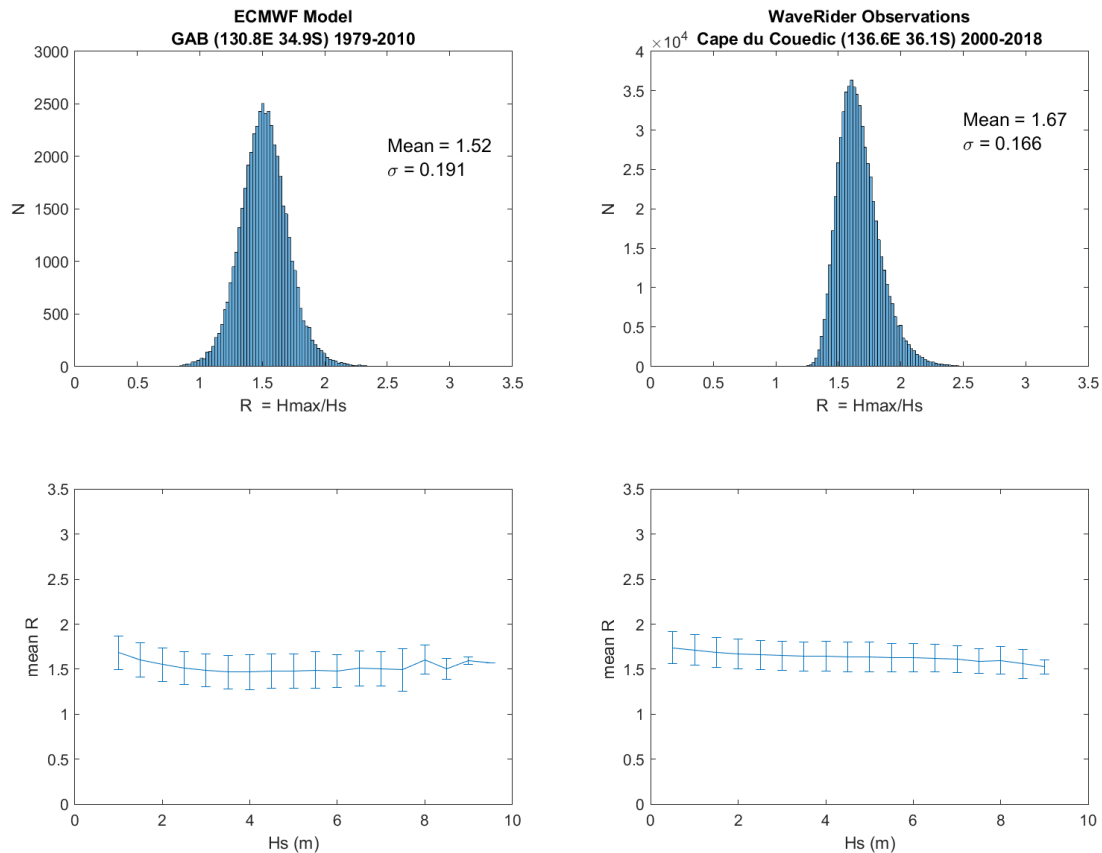


**Figure 35:** Top row: histograms of ratio of maximum wave height ( $H_{max}$ ) to significant wave height ( $H_s$ ) ( $R = H_{max}/H_s$ ) for model (Great Australian Bight, GAB) and observation (Cape du Couedic) sites. Bottom row: averaged  $R$  plotted as a function of  $H_s$  in 0.5 m bins, error bars indicate  $\pm$  one standard deviation ( $\sigma$ ).